



HAL
open science

Screening Sinkhorn Algorithm for Regularized Optimal Transport

Mokhtar Z. Alaya, Maxime Berar, Gilles Gasso, Alain Rakotomamonjy

► **To cite this version:**

Mokhtar Z. Alaya, Maxime Berar, Gilles Gasso, Alain Rakotomamonjy. Screening Sinkhorn Algorithm for Regularized Optimal Transport. Advances in Neural Information Processing Systems, 2019, Vancouver, Canada. hal-02142661v2

HAL Id: hal-02142661

<https://hal.science/hal-02142661v2>

Submitted on 21 Oct 2019 (v2), last revised 10 Feb 2020 (v3)

HAL is a multi-disciplinary open access archive for the deposit and dissemination of scientific research documents, whether they are published or not. The documents may come from teaching and research institutions in France or abroad, or from public or private research centers.

L'archive ouverte pluridisciplinaire **HAL**, est destinée au dépôt et à la diffusion de documents scientifiques de niveau recherche, publiés ou non, émanant des établissements d'enseignement et de recherche français ou étrangers, des laboratoires publics ou privés.

Screening Sinkhorn Algorithm for Regularized Optimal Transport

Mokhtar Z. Alaya

LITIS EA4108
University of Rouen Normandy
mokhtarzahdi.alaya@gmail.com

Maxime Bérar

LITIS EA4108
University of Rouen Normandy
maxime.berar@univ-rouen.fr

Gilles Gasso

LITIS EA4108
INSA, University of Rouen Normandy
gilles.gasso@insa-rouen.fr

Alain Rakotomamonjy

LITIS EA4108
University of Rouen Normandy
and Criteo AI Lab, Criteo Paris
alain.rakoto@insa-rouen.fr

Abstract

We introduce in this paper a novel strategy for efficiently approximating the Sinkhorn distance between two discrete measures. After identifying neglectable components of the dual solution of the regularized Sinkhorn problem, we propose to screen those components by directly setting them at that value before entering the Sinkhorn problem. This allows us to solve a smaller Sinkhorn problem while ensuring approximation with provable guarantees. More formally, the approach is based on a new formulation of *dual of Sinkhorn divergence problem* and on the KKT optimality conditions of this problem, which enable identification of dual components to be screened. This new analysis leads to the SCREENKHORN algorithm. We illustrate the efficiency of SCREENKHORN on complex tasks such as dimensionality reduction and domain adaptation involving regularized optimal transport.

1 Introduction

Computing optimal transport (OT) distances between pairs of probability measures or histograms, such as the earth mover’s distance [39, 34] and Monge-Kantorovich or Wasserstein distance [38], are currently generating an increasing attraction in different machine learning tasks [37, 28, 4, 22], statistics [18, 32, 14, 6, 17], and computer vision [8, 34, 36], among other applications [27, 33]. In many of these problems, OT exploits the geometric features of the objects at hand in the underlying spaces to be leveraged in comparing probability measures. This effectively leads to improved performance of methods that are oblivious to the geometry, for example the chi-squared distances or the Kullback-Leibler divergence. Unfortunately, this advantage comes at the price of an enormous computational cost of solving the OT problem, that can be prohibitive in large scale applications. For instance, the OT between two histograms with supports of equal size n can be formulated as a linear programming problem that requires generally super $\mathcal{O}(n^{2.5})$ [29] arithmetic operations, which is problematic when n becomes larger.

A remedy to the heavy computation burden of OT lies in a prevalent approach referred to as regularized OT [11] and operates by adding an entropic regularization penalty to the original problem. Such a regularization guarantees a unique solution, since the objective function is strongly convex, and a greater computational stability. More importantly, this regularized OT can be solved efficiently with celebrated matrix scaling algorithms, such as Sinkhorn’s fixed point iteration method [35, 26, 23].

Several works have considered further improvements in the resolution of this regularized OT problem. A greedy version of Sinkhorn algorithm, called Greenhorn [3], allows to select and update columns and rows that most violate the polytope constraints. Another approach based on low-rank approximation of the cost matrix using the Nyström method induces the Nys-Sink algorithm [2]. Other classical optimization algorithms have been considered for approximating the OT, for instance accelerated gradient descent [40, 13, 30], quasi-Newton methods [7, 12] and stochastic gradient descent [20, 1].

In this paper, we propose a novel technique for accelerating the Sinkhorn algorithm when computing regularized OT distance between discrete measures. Our idea is strongly related to a screening strategy when solving a *Lasso* problem in sparse supervised learning [21]. Based on the fact that a transport plan resulting from an OT problem is sparse or presents a large number of neglectable values [7], our objective is to identify the dual variables of an approximate Sinkhorn problem, that are smaller than a predefined threshold, and thus that can be safely removed before optimization while not altering too much the solution of the problem. Within this global context, our contributions are the following:

- From a methodological point of view, we propose a new formulation of the dual of the Sinkhorn divergence problem by imposing variables to be larger than a threshold. This formulation allows us to introduce sufficient conditions, computable beforehand, for a variable to strictly satisfy its constraint, leading then to a “screened” version of the dual of Sinkhorn divergence.
- We provide some theoretical analysis of the solution of the “screened” Sinkhorn divergence, showing that its objective value and the marginal constraint satisfaction are properly controlled as the number of screened variables decreases.
- From an algorithmic standpoint, we use a constrained L-BFGS-B algorithm [31, 9] but provide a careful analysis of the lower and upper bounds of the dual variables, resulting in a well-posed and efficient algorithm denoted as SCREENKHORN.
- Our empirical analysis depicts how the approach behaves in a simple Sinkhorn divergence computation context. When considered in complex machine learning pipelines, we show that SCREENKHORN can lead to strong gain in efficiency while not compromising on accuracy.

The remainder of the paper is organized as follow. In Section 2 we briefly review the basic setup of regularized discrete OT. Section 3 contains our main contribution, that is, the SCREENKHORN algorithm. Section 4 is devoted to theoretical guarantees for marginal violations of SCREENKHORN. In Section 5 we present numerical results for the proposed algorithm, compared with the state-of-art Sinkhorn algorithm as implemented in [16]. The proofs of theoretical results are postponed to the supplementary material as well as additional empirical results.

Notation. For any positive matrix $T \in \mathbb{R}^{n \times m}$, we define its entropy as $H(T) = -\sum_{i,j} T_{ij} \log(T_{ij})$. Let $r(T) = T\mathbf{1}_m \in \mathbb{R}^n$ and $c(T) = T^\top \mathbf{1}_n \in \mathbb{R}^m$ denote the rows and columns sums of T respectively. The coordinates $r_i(T)$ and $c_j(T)$ denote the i -th row sum and the j -th column sum of T , respectively. The scalar product between two matrices denotes the usual inner product, that is $\langle T, W \rangle = \text{tr}(T^\top W) = \sum_{i,j} T_{ij} W_{ij}$, where T^\top is the transpose of T . We write $\mathbf{1}$ (resp. $\mathbf{0}$) the vector having all coordinates equal to one (resp. zero). $\Delta(w)$ denotes the diag operator, such that if $w \in \mathbb{R}^n$, then $\Delta(w) = \text{diag}(w_1, \dots, w_n) \in \mathbb{R}^{n \times n}$. For a set of indices $L = \{i_1, \dots, i_k\} \subseteq \{1, \dots, n\}$ satisfying $i_1 < \dots < i_k$, we denote the complementary set of L by $L^c = \{1, \dots, n\} \setminus L$. We also denote $|L|$ the cardinality of L . Given a vector $w \in \mathbb{R}^n$, we denote $w_L = (w_{i_1}, \dots, w_{i_k})^\top \in \mathbb{R}^k$ and its complementary $w_{L^c} \in \mathbb{R}^{n-k}$. The notation is similar for matrices; given another subset of indices $S = \{j_1, \dots, j_l\} \subseteq \{1, \dots, m\}$ with $j_1 < \dots < j_l$, and a matrix $T \in \mathbb{R}^{n \times m}$, we use $T_{(L,S)}$, to denote the submatrix of T , namely the rows and columns of $T_{(L,S)}$ are indexed by L and S respectively. When applied to matrices and vectors, \odot and \oslash (Hadamard product and division) and exponential notations refer to elementwise operators. Given two real numbers a and b , we write $a \vee b = \max(a, b)$ and $a \wedge b = \min(a, b)$.

2 Regularized discrete OT

We briefly expose in this section the setup of OT between two discrete measures. We then consider the case when those distributions are only available through a finite number of samples, that is $\mu = \sum_{i=1}^n \mu_i \delta_{x_i} \in \Sigma_n$ and $\nu = \sum_{j=1}^m \nu_j \delta_{y_j} \in \Sigma_m$, where Σ_n is the probability simplex with n bins,

namely the set of probability vectors in \mathbb{R}_+^n , i.e., $\Sigma_n = \{w \in \mathbb{R}_+^n : \sum_{i=1}^n w_i = 1\}$. We denote their probabilistic couplings set as $\Pi(\mu, \nu) = \{P \in \mathbb{R}_+^{n \times m}, P\mathbf{1}_m = \mu, P^\top \mathbf{1}_n = \nu\}$.

Sinkhorn divergence. Computing OT distance between the two discrete measures μ and ν amounts to solving a linear problem [25] given by

$$\mathcal{S}(\mu, \nu) = \min_{P \in \Pi(\mu, \nu)} \langle C, P \rangle,$$

where $P = (P_{ij}) \in \mathbb{R}^{n \times m}$ is called the transportation plan, namely each entry P_{ij} represents the fraction of mass moving from x_i to y_j , and $C = (C_{ij}) \in \mathbb{R}^{n \times m}$ is a cost matrix comprised of nonnegative elements and related to the energy needed to move a probability mass from x_i to y_j . The entropic regularization of OT distances [11] relies on the addition of a penalty term as follows:

$$\mathcal{S}_\eta(\mu, \nu) = \min_{P \in \Pi(\mu, \nu)} \{\langle C, P \rangle - \eta H(P)\}, \quad (1)$$

where $\eta > 0$ is a regularization parameter. We refer to $\mathcal{S}_\eta(\mu, \nu)$ as the *Sinkhorn divergence* [11].

Dual of Sinkhorn divergence. Below we provide the derivation of the dual problem for the regularized OT problem (1). Towards this end, we begin with writing its Lagrangian dual function:

$$\mathcal{L}(P, w, z) = \langle C, P \rangle + \eta \langle \log P, P \rangle + \langle w, P\mathbf{1}_m - \mu \rangle + \langle z, P^\top \mathbf{1}_n - \nu \rangle.$$

The dual of Sinkhorn divergence can be derived by solving $\min_{P \in \mathbb{R}_+^{n \times m}} \mathcal{L}(P, w, z)$. It is easy to check that objective function $P \mapsto \mathcal{L}(P, w, z)$ is strongly convex and differentiable. Hence, one can solve the latter minimum by setting $\nabla_P \mathcal{L}(P, w, z)$ to $\mathbf{0}_{n \times m}$. Therefore, we get $P_{ij}^* = \exp(-\frac{1}{\eta}(w_i + z_j + C_{ij}) - 1)$, for all $i = 1, \dots, n$ and $j = 1, \dots, m$. Plugging this solution, and setting the change of variables $u = -w/\eta - 1/2$ and $v = -z/\eta - 1/2$, the dual problem is given by

$$\min_{u \in \mathbb{R}^n, v \in \mathbb{R}^m} \{\Psi(u, v) := \mathbf{1}_n^\top B(u, v) \mathbf{1}_m - \langle u, \mu \rangle - \langle v, \nu \rangle\}, \quad (2)$$

where $B(u, v) := \Delta(e^u) K \Delta(e^v)$ and $K := e^{-C/\eta}$ stands for the Gibbs kernel associated to the cost matrix C . We refer to problem (2) as the *dual of Sinkhorn divergence*. Then, the optimal solution P^* of the primal problem (1) takes the form $P^* = \Delta(e^{u^*}) K \Delta(e^{v^*})$ where the couple (u^*, v^*) satisfies:

$$(u^*, v^*) = \operatorname{argmin}_{u \in \mathbb{R}^n, v \in \mathbb{R}^m} \{\Psi(u, v)\}.$$

Note that the matrices $\Delta(e^{u^*})$ and $\Delta(e^{v^*})$ are unique up to a constant factor [35]. Moreover, P^* can be solved efficiently by iterative Bregman projections [5] referred to as Sinkhorn iterations, and the method is referred to as SINKHORN algorithm which, recently, has been proven to achieve a near- $\mathcal{O}(n^2)$ complexity [3].

3 Screened dual of Sinkhorn divergence

Motivation. The key idea of our approach is motivated by the so-called *static screening test* [21] in supervised learning, which is a method able to safely identify inactive features, i.e., features that have zero components in the solution vector. Then, these inactive features can be removed from the optimization problem to reduce its scale. Before diving into detailed algorithmic analysis, let us present a brief illustration of how we adapt static screening test to the dual of Sinkhorn divergence. Towards this end, we define the convex set $\mathcal{C}_\alpha^r \subseteq \mathbb{R}^r$, for $r \in \mathbb{N}$ and $\alpha > 0$, by $\mathcal{C}_\alpha^r = \{w \in \mathbb{R}^r : e^{w_i} \geq \alpha\}$. In Figure 1, we plot (e^{u^*}, e^{v^*}) where (u^*, v^*) is the pair solution of the dual of Sinkhorn divergence (2) in the particular case of: $n = m = 500, \eta = 1, \mu = \nu = \frac{1}{n} \mathbf{1}_n, x_i \sim \mathcal{N}((0, 0)^\top, \begin{pmatrix} 1 & 0 \\ 0 & 1 \end{pmatrix}), y_j \sim \mathcal{N}((3, 3)^\top, \begin{pmatrix} 1 & -0.8 \\ -0.8 & 1 \end{pmatrix})$ and the cost matrix C corresponds to the pairwise euclidean distance, i.e., $C_{ij} = \|x_i - y_j\|_2$. We also plot two lines corresponding to $e^{u^*} \equiv \alpha_u$ and $e^{v^*} \equiv \alpha_v$ for some $\alpha_u > 0$ and $\alpha_v > 0$, choosing randomly and playing the role of thresholds to select indices to be discarded. If we are able to identify these indices before solving the problem, they can be fixed at the thresholds and removed then from the optimization procedure yielding an approximate solution.

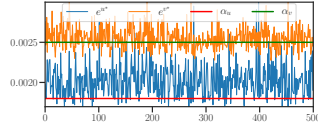


Figure 1: Plots of (e^{u^*}, e^{v^*}) with (u^*, v^*) is the pair solution of dual of Sinkhorn divergence (2) and the thresholds α_u, α_v .

Static screening test. Based on this idea, we define a so-called *approximate dual of Sinkhorn divergence*

$$\min_{u \in \mathcal{C}_{\frac{\varepsilon}{\kappa}}^n, v \in \mathcal{C}_{\varepsilon\kappa}^m} \{ \Psi_{\kappa}(u, v) := \mathbf{1}_n^\top B(u, v) \mathbf{1}_m - \langle \kappa u, \mu \rangle - \langle \frac{v}{\kappa}, \nu \rangle \}, \quad (3)$$

which is simply a dual of Sinkhorn divergence with lower-bounded variables, where the bounds are $\alpha_u = \varepsilon\kappa^{-1}$ and $\alpha_v = \varepsilon\kappa$ with $\varepsilon > 0$ and $\kappa > 0$ being fixed numeric constants which values will be clear later. The new formulation (3) has the form of $(\kappa\mu, \nu/\kappa)$ -scaling problem under constraints on the variables u and v . Those constraints make the problem significantly different from the standard scaling-problems [24]. We further emphasize that κ plays a key role in our screening strategy. Indeed, without κ , e^u and e^v can have inversely related scale that may lead in, for instance e^u being too large and e^v being too small, situation in which the screening test would apply only to coefficients of e^u or e^v and not for both of them. Moreover, it is clear that the approximate dual of Sinkhorn divergence coincides with the dual of Sinkhorn divergence (2) when $\varepsilon = 0$ and $\kappa = 1$. Intuitively, our hope is to gain efficiency in solving problem (3) compared to the original one in Equation (2) by avoiding optimization of variables smaller than the threshold and by identifying those that make the constraints active. More formally, the core of the static screening test aims at locating two subsets of indices (I, J) in $\{1, \dots, n\} \times \{1, \dots, m\}$ satisfying: $e^{u_i} > \alpha_u$, and $e^{v_j} > \alpha_v$, for all $(i, j) \in I \times J$ and $e^{u_{i'}} = \alpha_u$, and $e^{v_{j'}} = \alpha_v$, for all $(i', j') \in I^c \times J^c$, namely $(u, v) \in \mathcal{C}_{\alpha_u}^n \times \mathcal{C}_{\alpha_v}^m$. The following key result states sufficient conditions for identifying variables in I^c and J^c .

Lemma 1. *Let (u^*, v^*) be an optimal solution of problem (3). Define*

$$I_{\varepsilon, \kappa} = \{i = 1, \dots, n : \mu_i \geq \frac{\varepsilon^2}{\kappa} r_i(K)\}, J_{\varepsilon, \kappa} = \{j = 1, \dots, m : \nu_j \geq \kappa \varepsilon^2 c_j(K)\} \quad (4)$$

Then one has $e^{u_i^} = \varepsilon\kappa^{-1}$ and $e^{v_j^*} = \varepsilon\kappa$ for all $i \in I_{\varepsilon, \kappa}^c$ and $j \in J_{\varepsilon, \kappa}^c$.*

Proof of Lemma 1 is postponed to the supplementary material. It is worth to note that first order optimality conditions applied to (u^*, v^*) ensure that if $e^{u_i^*} > \varepsilon\kappa^{-1}$ then $e^{u_i^*} (K e^{v^*})_i = \kappa\mu_i$ and if $e^{v_j^*} > \varepsilon\kappa$ then $e^{v_j^*} (K^\top e^{u^*})_j = \kappa^{-1}\nu_j$, that correspond to the Sinkhorn marginal conditions [33] up to the scaling factor κ .

Screening with a fixed number budget of points. The approximate dual of Sinkhorn divergence is defined with respect to ε and κ . As those parameters are difficult to interpret, we exhibit their relations with a fixed number budget of points from the supports of μ and ν . In the sequel, we denote by $n_b \in \{1, \dots, n\}$ and $m_b \in \{1, \dots, m\}$ the number of points that are going to be optimized in problem (3), *i.e.*, the points we cannot guarantee that $e^{u_i^*} = \varepsilon\kappa^{-1}$ and $e^{v_j^*} = \varepsilon\kappa$.

Let us define $\xi \in \mathbb{R}^n$ and $\zeta \in \mathbb{R}^m$ to be the ordered decreasing vectors of $\mu \otimes r(K)$ and $\nu \otimes c(K)$ respectively, that is $\xi_1 \geq \xi_2 \geq \dots \geq \xi_n$ and $\zeta_1 \geq \zeta_2 \geq \dots \geq \zeta_m$. To keep only n_b -budget and m_b -budget of points, the parameters κ and ε satisfy $\varepsilon^2 \kappa^{-1} = \xi_{n_b}$ and $\varepsilon^2 \kappa = \zeta_{m_b}$. Hence

$$\varepsilon = (\xi_{n_b} \zeta_{m_b})^{1/4} \text{ and } \kappa = \sqrt{\frac{\zeta_{m_b}}{\xi_{n_b}}}. \quad (5)$$

This guarantees that $|I_{\varepsilon, \kappa}| = n_b$ and $|J_{\varepsilon, \kappa}| = m_b$ by construction. In addition, (n_b, m_b) tends to the full number budget of points (n, m) , when the couple parameters (ε, κ) converges to $(0, 1)$. In Figure 2, we plot these convergences, and hence the objective in problem (3) converges to the objective of dual of Sinkhorn divergence (2).

We are now in position to formulate the optimization problem related to the screened dual of Sinkhorn. Indeed, using the above analyses, any solution (u^*, v^*) of problem (3) satisfies $e^{u_i^*} \geq \varepsilon\kappa^{-1}$ and $e^{v_j^*} \geq \varepsilon\kappa$ for all $(i, j) \in (I_{\varepsilon, \kappa} \times J_{\varepsilon, \kappa})$, and $e^{u_i^*} = \varepsilon\kappa^{-1}$ and $e^{v_j^*} = \varepsilon\kappa$ for all $(i, j) \in (I_{\varepsilon, \kappa}^c \times J_{\varepsilon, \kappa}^c)$. Hence, we can restrict the problem (3) to variables in $I_{\varepsilon, \kappa}$ and $J_{\varepsilon, \kappa}$. This boils down to restricting the constraints feasibility $\mathcal{C}_{\frac{\varepsilon}{\kappa}}^n \cap \mathcal{C}_{\varepsilon\kappa}^m$ to the screened domain defined by $\mathcal{U}_{sc} \cap \mathcal{V}_{sc}$,

$$\mathcal{U}_{sc} = \{u \in \mathbb{R}^{n_b} : e^{u_{I_{\varepsilon, \kappa}}} \succeq \frac{\varepsilon}{\kappa} \mathbf{1}_{n_b}\} \text{ and } \mathcal{V}_{sc} = \{v \in \mathbb{R}^{m_b} : e^{v_{J_{\varepsilon, \kappa}}} \succeq \varepsilon\kappa \mathbf{1}_{m_b}\}$$

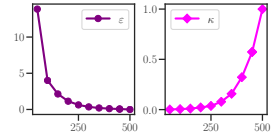


Figure 2: Plots of ε and κ as a function of number budget of points for a screening test with $n_b = m_b$ and the parameters μ, ν, η, C are set as in Figure (1). (ε, κ) tends to $(0, 1)$ as (n_b, m_b) tends to (n, m) .

where the vector comparison \succeq has to be understood elementwise. And, by replacing in Equation (3), the variables belonging to $(J_{\varepsilon,\kappa}^{\mathbf{G}} \times J_{\varepsilon,\kappa}^{\mathbf{G}})$ by $\varepsilon\kappa^{-1}$ and $\varepsilon\kappa$, we derive the *screened dual of Sinkhorn divergence problem* as

$$\min_{u \in \mathcal{U}_{\text{sc}}, v \in \mathcal{V}_{\text{sc}}} \{\Psi_{\varepsilon,\kappa}(u, v)\} \quad (6)$$

where

$$\begin{aligned} \Psi_{\varepsilon,\kappa}(u, v) = & (e^{u_{I_{\varepsilon,\kappa}}})^\top K_{(I_{\varepsilon,\kappa}, J_{\varepsilon,\kappa})} e^{v_{J_{\varepsilon,\kappa}}} + \varepsilon\kappa (e^{u_{I_{\varepsilon,\kappa}}})^\top K_{(I_{\varepsilon,\kappa}, J_{\varepsilon,\kappa}^{\mathbf{G}})} \mathbf{1}_{m_b} + \varepsilon\kappa^{-1} \mathbf{1}_{n_b}^\top K_{(J_{\varepsilon,\kappa}^{\mathbf{G}}, J_{\varepsilon,\kappa})} e^{v_{J_{\varepsilon,\kappa}}} \\ & - \kappa \mu_{I_{\varepsilon,\kappa}}^\top u_{I_{\varepsilon,\kappa}} - \kappa^{-1} \nu_{J_{\varepsilon,\kappa}}^\top v_{J_{\varepsilon,\kappa}} + \Xi \end{aligned}$$

$$\text{with } \Xi = \varepsilon^2 \sum_{i \in I_{\varepsilon,\kappa}^{\mathbf{G}}, j \in J_{\varepsilon,\kappa}^{\mathbf{G}}} K_{ij} - \kappa \log(\varepsilon\kappa^{-1}) \sum_{i \in I_{\varepsilon,\kappa}^{\mathbf{G}}} \mu_i - \kappa^{-1} \log(\varepsilon\kappa) \sum_{j \in J_{\varepsilon,\kappa}^{\mathbf{G}}} \nu_j.$$

The above problem uses only the restricted parts $K_{(I_{\varepsilon,\kappa}, J_{\varepsilon,\kappa})}$, $K_{(I_{\varepsilon,\kappa}, J_{\varepsilon,\kappa}^{\mathbf{G}})}$, and $K_{(J_{\varepsilon,\kappa}^{\mathbf{G}}, J_{\varepsilon,\kappa})}$ of the Gibbs kernel K for calculating the objective function $\Psi_{\varepsilon,\kappa}$. Hence, a gradient descent scheme will also need only those rows/columns of K . This is in contrast to Sinkhorn algorithm which performs alternating updates of all rows and columns of K . In summary, SCREENKHORN consists of two steps: the first one is a screening pre-processing providing the active sets $I_{\varepsilon,\kappa}$, $J_{\varepsilon,\kappa}$. The second one consists in solving Equation (6) using a constrained L-BFGS-B [9] for the stacked variable $\theta = (u_{I_{\varepsilon,\kappa}}, v_{J_{\varepsilon,\kappa}})$. Pseudocode of our proposed algorithm is shown in Algorithm 1. Note that in practice, we initialize the L-BFGS-B algorithm based on the output of a method, called RESTRICTED SINKHORN (see Algorithm 2 in the supplementary), which is a Sinkhorn-like algorithm applied to the active dual variables $\theta = (u_{I_{\varepsilon,\kappa}}, v_{J_{\varepsilon,\kappa}})$. While simple and efficient, the solution of this RESTRICTED SINKHORN algorithm does not satisfy the lower bound constraints of Problem (6) but provide a good candidate solution. Also note that L-BFGS-B handles box constraints on variables, but it becomes more efficient when these box bounds are carefully determined for problem (6). The following proposition (proof in supplementary material) expresses these bounds that are pre-calculated in the initialization step of SCREENKHORN.

Proposition 1. *Let $(u^{\text{sc}}, v^{\text{sc}})$ be an optimal pair solution of problem (6) and $K_{\min} = \min_{i \in I_{\varepsilon,\kappa}, j \in J_{\varepsilon,\kappa}} K_{ij}$.*

Then, one has

$$\frac{\varepsilon}{\kappa} \vee \frac{\min_{i \in I_{\varepsilon,\kappa}} \mu_i}{\varepsilon(m - m_b) + \varepsilon \vee \frac{\max_{j \in J_{\varepsilon,\kappa}} \nu_j}{n\varepsilon\kappa K_{\min}} m_b} \leq e^{u_i^{\text{sc}}} \leq \frac{\varepsilon}{\kappa} \vee \frac{\max_{i \in I_{\varepsilon,\kappa}} \mu_i}{m\varepsilon K_{\min}}, \quad (7)$$

and

$$\varepsilon\kappa \vee \frac{\min_{j \in J_{\varepsilon,\kappa}} \nu_j}{\varepsilon(n - n_b) + \varepsilon \vee \frac{\kappa \max_{i \in I_{\varepsilon,\kappa}} \mu_i}{m\varepsilon K_{\min}} n_b} \leq e^{v_j^{\text{sc}}} \leq \varepsilon\kappa \vee \frac{\max_{j \in J_{\varepsilon,\kappa}} \nu_j}{n\varepsilon K_{\min}} \quad (8)$$

for all $i \in I_{\varepsilon,\kappa}$ and $j \in J_{\varepsilon,\kappa}$.

4 Theoretical analysis and guarantees

This section is devoted to establishing theoretical guarantees for SCREENKHORN algorithm. We first define the screened marginals $\mu^{\text{sc}} = B(u^{\text{sc}}, v^{\text{sc}}) \mathbf{1}_m$ and $\nu^{\text{sc}} = B(u^{\text{sc}}, v^{\text{sc}})^\top \mathbf{1}_n$. Our first theoretical result, Proposition 2, gives an upper bound of the screened marginal violations with respect to ℓ_1 -norm.

Proposition 2. *Let $(u^{\text{sc}}, v^{\text{sc}})$ be an optimal pair solution of problem (6). Then one has*

$$\|\mu - \mu^{\text{sc}}\|_1^2 = \mathcal{O}\left(n_b c_\kappa + (n - n_b) \left(\frac{\|C\|_\infty}{\eta} + \frac{m_b}{\sqrt{nm} c_{\mu\nu} K_{\min}^{3/2}} + \frac{m - m_b}{\sqrt{nm} K_{\min}} + \log\left(\frac{\sqrt{nm}}{m_b c_{\mu\nu}^{5/2}}\right)\right)\right) \quad (9)$$

and

$$\|\nu - \nu^{\text{sc}}\|_1^2 = \mathcal{O}\left(m_b c_{\frac{1}{\kappa}} + (m - m_b) \left(\frac{\|C\|_\infty}{\eta} + \frac{n_b}{\sqrt{nm} c_{\mu\nu} K_{\min}^{3/2}} + \frac{n - n_b}{\sqrt{nm} K_{\min}} + \log\left(\frac{\sqrt{nm}}{n_b c_{\mu\nu}^{5/2}}\right)\right)\right), \quad (10)$$

where $c_z = z - \log z - 1$ for $z > 0$ and $c_{\mu\nu} = \underline{\mu} \wedge \underline{\nu}$ with $\underline{\mu} = \min_{i \in I_{\varepsilon,\kappa}} \mu_i$ and $\underline{\nu} = \min_{j \in J_{\varepsilon,\kappa}} \nu_j$.

Algorithm 1: SCREENKHORN($C, \eta, \mu, \nu, n_b, m_b$)

Step 1: Screening pre-processing

1. $\xi \leftarrow \text{sort}(\mu \otimes r(K)), \zeta \leftarrow \text{sort}(\nu \otimes c(K)); //(\text{decreasing order})$
2. $\varepsilon \leftarrow (\xi_{n_b} \zeta_{m_b})^{1/4}, \kappa \leftarrow \sqrt{\zeta_{m_b} / \xi_{n_b}}$;
3. $I_{\varepsilon, \kappa} \leftarrow \{i = 1, \dots, n : \mu_i \geq \varepsilon^2 \kappa^{-1} r_i(K)\}, J_{\varepsilon, \kappa} \leftarrow \{j = 1, \dots, m : \nu_j \geq \varepsilon^2 \kappa c_j(K)\}$;
4. $\underline{\mu} \leftarrow \min_{i \in I_{\varepsilon, \kappa}} \mu_i, \bar{\mu} \leftarrow \max_{i \in I_{\varepsilon, \kappa}} \mu_i, \underline{\nu} \leftarrow \min_{j \in J_{\varepsilon, \kappa}} \nu_j, \bar{\nu} \leftarrow \max_{j \in J_{\varepsilon, \kappa}} \nu_j$;
5. $\underline{u} \leftarrow \log\left(\frac{\varepsilon}{\kappa} \vee \frac{\underline{\mu}}{\varepsilon(m-m_b) + \varepsilon \sqrt{\frac{\bar{\nu}}{n \varepsilon \kappa K_{\min}} m_b}}\right), \bar{u} \leftarrow \log\left(\frac{\varepsilon}{\kappa} \vee \frac{\bar{\mu}}{m \varepsilon K_{\min}}\right)$;
6. $\underline{v} \leftarrow \log\left(\varepsilon \kappa \vee \frac{\underline{\nu}}{\varepsilon(n-n_b) + \varepsilon \sqrt{\frac{\kappa \bar{\mu}}{m \varepsilon K_{\min}} n_b}}\right), \bar{v} \leftarrow \log\left(\varepsilon \kappa \vee \frac{\bar{\nu}}{n \varepsilon K_{\min}}\right)$;
7. $\bar{\theta} \leftarrow \text{stack}(\bar{u} \mathbf{1}_{n_b}, \bar{v} \mathbf{1}_{m_b}), \underline{\theta} \leftarrow \text{stack}(\underline{u} \mathbf{1}_{n_b}, \underline{v} \mathbf{1}_{m_b})$;

Step 2: L-BFGS-B solver on the screened variables

8. $u^{(0)} \leftarrow \log(\varepsilon \kappa^{-1}) \mathbf{1}_{n_b}, v^{(0)} \leftarrow \log(\varepsilon \kappa) \mathbf{1}_{m_b}$;
 9. $\hat{u}, \hat{v} \leftarrow \text{RESTRICTED SINKHORN}(u^{(0)}, v^{(0)}), \theta^{(0)} \leftarrow \text{stack}(\hat{u}, \hat{v})$;
 10. $\theta \leftarrow \text{L-BFGS-B}(\theta^{(0)}, \underline{\theta}, \bar{\theta})$;
 11. $\theta_u \leftarrow (\theta_1, \dots, \theta_{n_b})^\top, \theta_v \leftarrow (\theta_{n_b+1}, \dots, \theta_{n_b+m_b})^\top$;
 12. $u_i^{\text{sc}} \leftarrow (\theta_u)_i$ if $i \in I_{\varepsilon, \kappa}$ and $u_i \leftarrow \log(\varepsilon \kappa^{-1})$ if $i \in I_{\varepsilon, \kappa}^c$;
 13. $v_j^{\text{sc}} \leftarrow (\theta_v)_j$ if $j \in J_{\varepsilon, \kappa}$ and $v_j \leftarrow \log(\varepsilon \kappa)$ if $j \in J_{\varepsilon, \kappa}^c$;
 14. **return** $B(u^{\text{sc}}, v^{\text{sc}})$.
-

Proof of Proposition 2 is presented in supplementary material and it is based on first order optimality conditions for problem (6) and on a generalization of Pinsker inequality (see Lemma 2 in supplementary). Note that c_κ and c_\perp tend to zeros as κ goes to one, which is the case when the number budget of points (n_b, m_b) tends to the full one (n, m) .

Our second theoretical result, Proposition 3, is an upper bound of the difference between objective values of SCREENKHORN and dual of Sinkhorn divergence (2).

Proposition 3. *Let $(u^{\text{sc}}, v^{\text{sc}})$ be an optimal pair solution of problem (6) and (u^*, v^*) is the pair solution of dual of Sinkhorn divergence (2). Then we have*

$$\Psi_{\varepsilon, \kappa}(u^{\text{sc}}, v^{\text{sc}}) - \Psi(u^*, v^*) = \mathcal{O}(R(\|\mu - \mu^{\text{sc}}\|_1 + \|\nu - \nu^{\text{sc}}\|_1 + \omega_\kappa)).$$

where $R = \frac{\|C\|_\infty}{\eta} + \log\left(\frac{(n \vee m)^2}{n m c_{\mu\nu}}\right)$ and $\omega_\kappa = (1 - \kappa)\|\mu^{\text{sc}}\|_1 + (\kappa^{-1} - 1)\|\nu^{\text{sc}}\|_1 + \kappa^{-1} - \kappa$.

Proof of Proposition 3 is exposed in the supplementary material. Comparing to some other analysis results of this quantity, see for instance Lemma 2 in [13] and Lemma 3.1 in [30], our bound involves an additional term ω_κ (with $\omega_1 = 0$), that tends to zero as the pair budget (n_b, m_b) goes to the full number budget of points (n, m) (i.e., κ goes to 1). To better characterize ω_κ , a control of the ℓ_1 -norms of the screened marginals μ^{sc} and ν^{sc} are given in Lemma 3 in the supplementary material.

5 Numerical experiments

In this section, we present some numerical analyses of our SCREENKHORN algorithm and show how it behaves when integrated into some complex machine learning pipelines.

5.1 Setup

We have implemented our SCREENKHORN algorithm in Python and used the L-BFGS-B of Scipy. Regarding the machine-learning based comparison, we have based our code on the ones of Python Optimal Transport toolbox (POT) [16] and just replaced the `sinkhorn` function call with a `screenkhorn` one. We have considered the POT's default SINKHORN stopping criterion parameters and for SCREENKHORN, the L-BFGS-B algorithm is stopped when the largest component of the projected gradient is smaller than 10^{-6} , when the number of iterations or the number of objective function evaluations reach 10^5 . For all applications, we have set $\eta = 1$ unless otherwise specified.

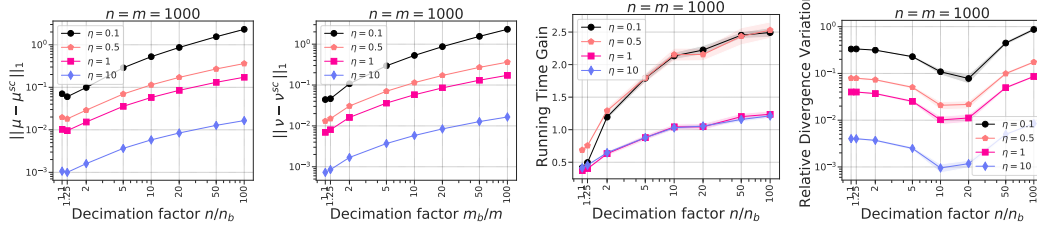


Figure 3: Empirical evaluation of SCREENKHORN vs SINKHORN for normalized cost matrix *i.e.* $\|C\|_\infty = 1$. (most-left): marginal violations in relation with the budget of points on n and m . (center-right) ratio of computation times $\frac{T_{\text{SINKHORN}}}{T_{\text{SCREENKHORN}}}$ and, (right) relative divergence variation. The results are averaged over 30 trials.

5.2 Analysing on toy problem

We compare SCREENKHORN to SINKHORN as implemented in POT toolbox¹ on a synthetic example. The dataset we use consists of source samples generated from a bi-dimensional gaussian mixture and target samples following the same distribution but with different gaussian means. We consider an unsupervised domain adaptation using optimal transport with entropic regularization. Several settings are explored: different values of η , the regularization parameter, the allowed budget $\frac{n_b}{n} = \frac{m_b}{m}$ ranging from 0.01 to 0.99, different values of n and m . We empirically measure marginal violations as the norms $\|\mu - \mu^{\text{sc}}\|_1$ and $\|\nu - \nu^{\text{sc}}\|_1$, running time expressed as $\frac{T_{\text{SINKHORN}}}{T_{\text{SCREENKHORN}}}$ and the relative divergence difference $|\langle C, P^* \rangle - \langle C, P^{\text{sc}} \rangle| / \langle C, P^* \rangle$ between SCREENKHORN and SINKHORN, where $P^* = \Delta(e^{u^*})K\Delta(e^{v^*})$ and $P^{\text{sc}} = \Delta(e^{u^{\text{sc}}})K\Delta(e^{v^{\text{sc}}})$. Figure 3 summarizes the observed behaviors of both algorithms under these settings. We choose to only report results for $n = m = 1000$ as we get similar findings for other values of n and m .

SCREENKHORN provides good approximation of the marginals μ and ν for “high” values of the regularization parameter η ($\eta > 1$). The approximation quality diminishes for small η . As expected $\|\mu - \mu^{\text{sc}}\|_1$ and $\|\nu - \nu^{\text{sc}}\|_1$ converge towards zero when increasing the budget of points. Remarkably marginal violations are almost negligible whatever the budget for high η . According to computation gain, SCREENKHORN is almost 2 times faster than SINKHORN at high decimation factor n/n_b (low budget) while the reverse holds when n/n_b gets close to 1. Computational benefit of SCREENKHORN also depends on η with appropriate values $\eta \leq 1$. Finally except for $\eta = 0.1$ SCREENKHORN achieves a divergence $\langle C, P \rangle$ close to the one of Sinkhorn showing that our static screening test provides a reasonable approximation of the Sinkhorn divergence. As such, we believe that SCREENKHORN will be practically useful in cases where modest accuracy on the divergence is sufficient. This may be the case of a loss function for a gradient descent method (see next section).

5.3 Integrating SCREENKHORN into machine learning pipelines

Here, we analyse the impact of using SCREENKHORN instead of SINKHORN in a complex machine learning pipeline. Our two applications are a dimensionality reduction technique, denoted as Wasserstein Discriminant Analysis (WDA), based on Wasserstein distance approximated through Sinkhorn divergence [17] and a domain-adaptation using optimal transport mapping [10], named OTDA.

WDA aims at finding a linear projection which minimize the ratio of distance between intra-class samples and distance inter-class samples, where the distance is understood in a Sinkhorn divergence sense. We have used a toy problem involving Gaussian classes with 2 discriminative features and 8 noisy features and the MNIST dataset. For the former problem, we aim at find the best two-dimensional linear subspace in a WDA sense whereas for MNIST, we look for a subspace of dimension 20 starting from the original 728 dimensions. Quality of the retrieved subspace are evaluated using classification task based on a 1-nearest neighbour approach.

Figure 4 presents the average gain (over 30 trials) in computational time we get as the number of examples evolve and for different decimation factors of the SCREENKHORN problem. Analysis of

¹<https://pot.readthedocs.io/en/stable/index.html>

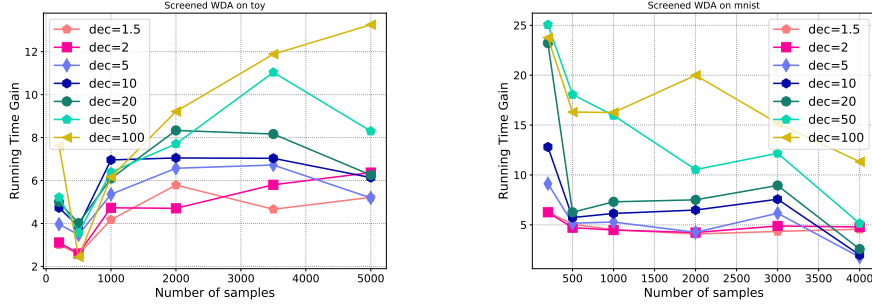


Figure 4: Wasserstein Discriminant Analysis : running time gain for (left) a toy dataset and (right) MNIST as a function of the number of examples and the data decimation factor in SCREENKHORN.

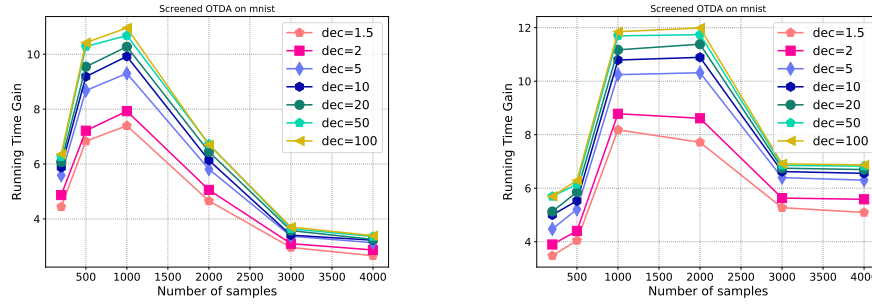


Figure 5: OT Domain adaptation : running time gain for MNIST as a function of the number of examples and the data decimation factor in SCREENKHORN. Group-lasso hyperparameter values (left) 1. (right) 10.

the quality of the subspace have been reported to the supplementary material (see Figure 7), but we can remark a small loss of performance of SCREENKHORN for the toy problem, while for MNIST, accuracies are equivalent regardless of the decimation factor. We can note that the minimal gains are respectively 2 and 4.5 for the toy and MNIST problem whereas the maximal gain for 4000 samples is slightly larger than an order of magnitude.

For the OT based domain adaptation problem, we have considered the OTDA with $\ell_{\frac{1}{2},1}$ group-lasso regularizer that helps in exploiting available labels in the source domain. The problem is solved using a majorization-minimization approach for handling the non-convexity of the problem. Hence, at each iteration, a SINKHORN/SCREENKHORN has to be computed and the number of iteration is sensitive to the regularizer strength. As a domain-adaptation problem, we have used a MNIST to USPS problem in which features have been computed from the first layers of a domain adversarial neural networks [19] before full convergence of the networks (so as to leave room for OT adaptation). Figure 5 reports the gain in running time for 2 different values of the group-lasso regularizer hyperparameter, while the curves of performances are reported in the supplementary material. We can note that for all the SCREENKHORN with different decimation factors, the gain in computation goes from a factor of 4 to 12, without any loss of the accuracy performance.

6 Conclusion

The paper introduces a novel efficient approximation of the Sinkhorn divergence based on a screening strategy. Screening some of the Sinkhorn dual variables has been made possible by defining a novel constrained dual problem and by carefully analyzing its optimality conditions. From the latter, we derived some sufficient conditions depending on the ground cost matrix, that some dual variables are smaller than a given threshold. Hence, we need just to solve a restricted dual Sinkhorn problem using an off-the-shelf L-BFGS-B algorithm. We also provide some theoretical guarantees of the quality of the approximation with respect to the number of variables that have been screened. Numerical experiments show the behaviour of our SCREENKHORN algorithm and computational time gain it can achieve when integrated in some complex machine learning pipelines.

Acknowledgments

This work was supported by grants from the Normandie Projet GRR-DAISI, European funding FEDER DAISI and OATMIL ANR-17-CE23-0012 Project of the French National Research Agency (ANR).

References

- [1] B. K. Abid and R. Gower. Stochastic algorithms for entropy-regularized optimal transport problems. In Amos Storkey and Fernando Perez-Cruz, editors, *Proceedings of the Twenty-First International Conference on Artificial Intelligence and Statistics*, volume 84 of *Proceedings of Machine Learning Research*, pages 1505–1512, Playa Blanca, Lanzarote, Canary Islands, 2018. PMLR.
- [2] J. Altschuler, F. Bach, A. Rudi, and J. Weed. Massively scalable Sinkhorn distances via the Nyström method, 2018.
- [3] J. Altschuler, J. Weed, and P. Rigollet. Near-linear time approximation algorithms for optimal transport via Sinkhorn iteration. In *Proceedings of the 31st International Conference on Neural Information Processing Systems*, NIPS17, pages 1961–1971, USA, 2017. Curran Associates Inc.
- [4] M. Arjovsky, S. Chintala, and L. Bottou. Wasserstein generative adversarial networks. In Doina Precup and Yee Whye Teh, editors, *Proceedings of the 34th International Conference on Machine Learning*, volume 70 of *Proceedings of Machine Learning Research*, pages 214–223, International Convention Centre, Sydney, Australia, 2017. PMLR.
- [5] J. D. Benamou, G. Carlier, M. Cuturi, L. Nenna, and G. Peyré. Iterative bregman projections for regularized transportation problems. *SIAM J. Scientific Computing*, 37, 2015.
- [6] J. Bigot, R. Gouet, T. Klein, and A. López. Geodesic PCA in the Wasserstein space by convex PCA. *Ann. Inst. H. Poincaré Probab. Statist.*, 53(1):1–26, 2017.
- [7] M. Blondel, V. Seguy, and A. Rolet. Smooth and sparse optimal transport. In Amos Storkey and Fernando Perez-Cruz, editors, *Proceedings of the Twenty-First International Conference on Artificial Intelligence and Statistics*, volume 84 of *Proceedings of Machine Learning Research*, pages 880–889, Playa Blanca, Lanzarote, Canary Islands, 2018. PMLR.
- [8] N. Bonneel, M. van de Panne, S. Paris, and W. Heidrich. Displacement interpolation using Lagrangian mass transport. *ACM Trans. Graph.*, 30(6):158:1–158:12, 2011.
- [9] R. Byrd, P. Lu, J. Nocedal, and C. Zhu. A limited memory algorithm for bound constrained optimization. *SIAM Journal on Scientific Computing*, 16(5):1190–1208, 1995.
- [10] Nicolas Courty, Rémi Flamary, Devis Tuia, and Alain Rakotomamonjy. Optimal transport for domain adaptation. *IEEE transactions on pattern analysis and machine intelligence*, 39(9):1853–1865, 2017.
- [11] M. Cuturi. Sinkhorn distances: Lightspeed computation of optimal transport. In C. J. C. Burges, L. Bottou, M. Welling, Z. Ghahramani, and K. Q. Weinberger, editors, *Advances in Neural Information Processing Systems 26*, pages 2292–2300. Curran Associates, Inc., 2013.
- [12] M. Cuturi and G. Peyré. A smoothed dual approach for variational Wasserstein problems. *SIAM Journal on Imaging Sciences*, 9(1):320–343, 2016.
- [13] P. Dvurechensky, A. Gasnikov, and A. Kroshnin. Computational optimal transport: Complexity by accelerated gradient descent is better than by Sinkhorn’s algorithm. In Jennifer Dy and Andreas Krause, editors, *Proceedings of the 35th International Conference on Machine Learning*, volume 80 of *Proceedings of Machine Learning Research*, pages 1367–1376, Stockholmsmässan, Stockholm Sweden, 2018. PMLR.
- [14] J. Ebert, V. Spokoiny, and A. Suvorikova. Construction of non-asymptotic confidence sets in 2-Wasserstein space, 2017.
- [15] Y. Fei, G. Rong, B. Wang, and W. Wang. Parallel L-BFGS-B algorithm on GPU. *Computers and Graphics*, 40:1 – 9, 2014.
- [16] R. Flamary and N. Courty. POT: Python optimal transport library, 2017.
- [17] R. Flamary, M. Cuturi, N. Courty, and A. Rakotomamonjy. Wasserstein discriminant analysis. *Machine Learning*, 107(12):1923–1945, 2018.

- [18] C. Frogner, C. Zhang, H. Mobahi, M. Araya, and T. A. Poggio. Learning with a Wasserstein loss. In C. Cortes, N. D. Lawrence, D. D. Lee, M. Sugiyama, and R. Garnett, editors, *Advances in Neural Information Processing Systems 28*, pages 2053–2061. Curran Associates, Inc., 2015.
- [19] Y. Ganin, E. Ustinova, H. Ajakan, P. Germain, H. Larochelle, F. Laviolette, M. Marchand, and V. Lempitsky. Domain-adversarial training of neural networks. *The Journal of Machine Learning Research*, 17(1):2096–2030, 2016.
- [20] A. Genevay, M. Cuturi, G. Peyré, and F. Bach. Stochastic optimization for large-scale optimal transport. In D. D. Lee, M. Sugiyama, U. V. Luxburg, I. Guyon, and R. Garnett, editors, *Advances in Neural Information Processing Systems 29*, pages 3440–3448. Curran Associates, Inc., 2016.
- [21] L. El Ghaoui, V. Viallon, and T. Rabbani. Safe feature elimination in sparse supervised learning. *CoRR*, abs/1009.4219, 2010.
- [22] N. Ho, X. L. Nguyen, M. Yurochkin, H. H. Bui, V. Huynh, and D. Phung. Multilevel clustering via Wasserstein means. In *Proceedings of the 34th International Conference on Machine Learning - Volume 70*, ICML’17, pages 1501–1509. JMLR.org, 2017.
- [23] B. Kalantari, I. Lari, F. Ricca, and B. Simeone. On the complexity of general matrix scaling and entropy minimization via the ras algorithm. *Mathematical Programming*, 112(2):371–401, 2008.
- [24] B. Kalantari and L. Khachiyan. On the complexity of nonnegative-matrix scaling. *Linear Algebra and its Applications*, 240:87 – 103, 1996.
- [25] L. Kantorovich. On the transfer of masses (in russian). *Doklady Akademii Nauk*, 2:227–229, 1942.
- [26] P. Knight. The Sinkhorn–Knopp algorithm: Convergence and applications. *SIAM Journal on Matrix Analysis and Applications*, 30(1):261–275, 2008.
- [27] S. Kolouri, S. R. Park, M. Thorpe, D. Slepcev, and G. K. Rohde. Optimal mass transport: Signal processing and machine-learning applications. *IEEE Signal Processing Magazine*, 34(4):43–59, 2017.
- [28] M. Kusner, Y. Sun, N. Kolkin, and K. Weinberger. From word embeddings to document distances. In Francis Bach and David Blei, editors, *Proceedings of the 32nd International Conference on Machine Learning*, volume 37 of *Proceedings of Machine Learning Research*, pages 957–966, Lille, France, 2015. PMLR.
- [29] Y. T. Lee and A. Sidford. Path finding methods for linear programming: Solving linear programs in $\tilde{O}(\text{vrank})$ iterations and faster algorithms for maximum flow. In *Proceedings of the 2014 IEEE 55th Annual Symposium on Foundations of Computer Science*, FOCS ’14, pages 424–433, Washington, DC, USA, 2014. IEEE Computer Society.
- [30] T. Lin, N. Ho, and M. I. Jordan. On efficient optimal transport: An analysis of greedy and accelerated mirror descent algorithms. *CoRR*, abs/1901.06482, 2019.
- [31] J. Nocedal. Updating quasi-newton matrices with limited storage. *Mathematics of Computation*, 35(151):773–782, 1980.
- [32] V. M. Panaretos and Y. Zemel. Amplitude and phase variation of point processes. *Ann. Statist.*, 44(2):771–812, 2016.
- [33] G. Peyré and M. Cuturi. Computational optimal transport. *Foundations and Trends® in Machine Learning*, 11(5-6):355–607, 2019.
- [34] Y. Rubner, C. Tomasi, and L. J. Guibas. The earth mover’s distance as a metric for image retrieval. *International Journal of Computer Vision*, 40(2):99–121, 2000.
- [35] R. Sinkhorn. Diagonal equivalence to matrices with prescribed row and column sums. *The American Mathematical Monthly*, 74(4):402–405, 1967.
- [36] J. Solomon, F. de Goes, G. Peyré, M. Cuturi, A. Butscher, A. Nguyen, T. Du, and L. Guibas. Convolutional Wasserstein distances: Efficient optimal transportation on geometric domains. *ACM Trans. Graph.*, 34(4):66:1–66:11, 2015.
- [37] J. Solomon, R. Rustamov, L. Guibas, and A. Butscher. Wasserstein propagation for semi-supervised learning. In Eric P. Xing and Tony Jebara, editors, *Proceedings of the 31st International Conference on Machine Learning*, volume 32 of *Proceedings of Machine Learning Research*, pages 306–314, Beijing, China, 2014. PMLR.

- [38] C. Villani. *Optimal Transport: Old and New*, volume 338 of *Grundlehren der mathematischen Wissenschaften*. Springer Berlin Heidelberg, 2009.
- [39] M. Werman, S. Peleg, and A. Rosenfeld. A distance metric for multidimensional histograms. *Computer Vision, Graphics, and Image Processing*, 32(3):328 – 336, 1985.
- [40] Y. Xie, X. Wang, R. Wang, and H. Zha. A fast proximal point method for computing Wasserstein distance, 2018.

7 Supplementary material

7.1 Proof of Lemma 1

Since the objective function Ψ_κ is convex with respect to (u, v) , the set of optima of problem (3) is non empty. Introducing two dual variables $\lambda \in \mathbb{R}_+^n$ and $\beta \in \mathbb{R}_+^m$ for each constraint, the Lagrangian of problem (3) reads as

$$\mathcal{L}(u, v, \lambda, \beta) = \frac{\varepsilon}{\kappa} \langle \lambda, \mathbf{1}_n \rangle + \varepsilon \kappa \langle \beta, \mathbf{1}_m \rangle + \mathbf{1}_n^\top B(u, v) \mathbf{1}_m - \langle \kappa u, \mu \rangle - \left\langle \frac{v}{\kappa}, \nu \right\rangle - \langle \lambda, e^u \rangle - \langle \beta, e^v \rangle$$

First order conditions then yield that the Lagrangian multipliers solutions λ^* and β^* satisfy

$$\begin{aligned} \nabla_u \mathcal{L}(u^*, v^*, \lambda^*, \beta^*) &= e^{u^*} \odot (K e^{v^*} - \lambda^*) - \kappa \mu = \mathbf{0}_n, \\ \text{and } \nabla_v \mathcal{L}(u^*, v^*, \lambda^*, \beta^*) &= e^{v^*} \odot (K^\top e^{u^*} - \beta) - \frac{\nu}{\kappa} = \mathbf{0}_m \end{aligned}$$

which leads to

$$\lambda^* = K e^{v^*} - \kappa \mu \odot e^{u^*} \text{ and } \beta^* = K^\top e^{u^*} - \nu \odot \kappa e^{v^*}$$

For all $i = 1, \dots, n$ we have that $e^{u_i^*} \geq \frac{\varepsilon}{\kappa}$. Further, the condition on the dual variable $\lambda_i^* > 0$ ensures that $e^{u_i^*} = \frac{\varepsilon}{\kappa}$ and hence $i \in I_{\varepsilon, \kappa}^{\mathbf{G}}$. We have that $\lambda_i^* > 0$ is equivalent to $e^{u_i^*} r_i(K) e^{v_j^*} > \kappa \mu_i$ which is satisfied when $\varepsilon^2 r_i(K) > \kappa \mu_i$. In a symmetric way we can prove the same statement for $e^{v_j^*}$.

7.2 Proof of Proposition 1

We prove only the first statement (7) and similarly we can prove the second one (8). For all $i \in I_{\varepsilon, \kappa}$, we have $e^{u_i^{\text{sc}}} > \frac{\varepsilon}{\kappa}$ or $e^{u_i^{\text{sc}}} = \frac{\varepsilon}{\kappa}$. In one hand, if $e^{u_i^{\text{sc}}} > \frac{\varepsilon}{\kappa}$ then according to the optimality conditions $\lambda_i^{\text{sc}} = 0$, which implies $e^{u_i^{\text{sc}}} \sum_{j=1}^m K_{ij} e^{v_j^{\text{sc}}} = \kappa \mu_i$. In another hand, we have

$$e^{u_i^{\text{sc}}} \min_{i,j} K_{ij} \sum_{j=1}^m e^{v_j^{\text{sc}}} \leq e^{u_i^{\text{sc}}} \sum_{j=1}^m K_{ij} e^{v_j^{\text{sc}}} = \kappa \mu_i.$$

We further observe that $\sum_{j=1}^m e^{v_j^{\text{sc}}} = \sum_{j \in J_{\varepsilon, \kappa}} e^{v_j^{\text{sc}}} + \sum_{j \in J_{\varepsilon, \kappa}^{\mathbf{G}}} e^{v_j^{\text{sc}}} \geq \varepsilon \kappa |J_{\varepsilon, \kappa}| + \varepsilon \kappa |J_{\varepsilon, \kappa}^{\mathbf{G}}| = \varepsilon \kappa m$. Then

$$\max_{i \in I_{\varepsilon, \kappa}} e^{u_i^{\text{sc}}} \leq \frac{\varepsilon}{\kappa} \vee \frac{\max_{i \in I_{\varepsilon, \kappa}} \mu_i}{m \varepsilon K_{\min}}.$$

Analogously, one can obtain for all $j \in J_{\varepsilon, \kappa}$

$$\max_{j \in J_{\varepsilon, \kappa}} e^{v_j^{\text{sc}}} \leq \varepsilon \kappa \vee \frac{\max_{j \in J_{\varepsilon, \kappa}} \nu_j}{n \varepsilon K_{\min}}. \quad (11)$$

Now, since $K_{ij} \leq 1$, we have

$$e^{u_i^{\text{sc}}} \sum_{j=1}^m e^{v_j^{\text{sc}}} \geq e^{u_i^{\text{sc}}} \sum_{j=1}^m K_{ij} e^{v_j^{\text{sc}}} = \kappa \mu_i.$$

Using (11), we get

$$\sum_{j=1}^m e^{v_j^{\text{sc}}} = \sum_{j \in J_{\varepsilon, \kappa}} e^{v_j^{\text{sc}}} + \sum_{j \in J_{\varepsilon, \kappa}^{\mathbf{G}}} e^{v_j^{\text{sc}}} \leq \varepsilon \kappa |J_{\varepsilon, \kappa}^{\mathbf{G}}| + \varepsilon \kappa \vee \frac{\max_{j \in J_{\varepsilon, \kappa}} \nu_j}{n \varepsilon K_{\min}} |J_{\varepsilon, \kappa}|.$$

Therefore,

$$\min_{i \in I_{\varepsilon, \kappa}} e^{u_i^{\text{sc}}} \geq \frac{\varepsilon}{\kappa} \vee \frac{\kappa \min_{i \in I_{\varepsilon, \kappa}} \mu_i}{\varepsilon \kappa (m - m_b) + \varepsilon \kappa \vee \frac{\max_{j \in J_{\varepsilon, \kappa}} \nu_j}{n \varepsilon K_{\min}} m_b}.$$

7.3 Proof of Proposition 2

We define the distance function $\varrho : \mathbb{R}_+ \times \mathbb{R}_+ \mapsto [0, \infty]$ by $\varrho(a, b) = b - a + a \log(\frac{a}{b})$. While ϱ is not a metric, it is easy to see that ϱ is not nonnegative and satisfies $\varrho(a, b) = 0$ iff $a = b$. The violations are computed through the following function:

$$d_\varrho(\gamma, \beta) = \sum_{i=1}^n \varrho(\gamma_i, \beta_i), \text{ for } \gamma, \beta \in \mathbb{R}_+^n.$$

Note that if γ, β are two vectors of positive entries, $d_\varrho(\gamma, \beta)$ will return some measurement on how far they are from each other. The next Lemma is from [1] (see Lemma 7 herein).

Lemma 2. For any $\gamma, \beta \in \mathbb{R}_+^n$, the following generalized Pinsker inequality holds

$$\|\gamma - \beta\|_1 \leq \sqrt{7(\|\gamma\|_1 \wedge \|\beta\|_1)d_\rho(\gamma, \beta)}.$$

The optimality conditions for $(u^{\text{sc}}, v^{\text{sc}})$ entails

$$\mu_i^{\text{sc}} = \begin{cases} e^{u_i^{\text{sc}}} \sum_{j=1}^m K_{ij} e^{v_j^{\text{sc}}}, & \text{if } i \in I_{\varepsilon, \kappa}, \\ \frac{\varepsilon}{\kappa} \sum_{j=1}^m K_{ij} e^{v_j^{\text{sc}}}, & \text{if } i \in J_{\varepsilon, \kappa}^{\mathbf{G}}, \end{cases} = \begin{cases} \kappa \mu_i, & \text{if } i \in I_{\varepsilon, \kappa}, \\ \frac{\varepsilon}{\kappa} \sum_{j=1}^m K_{ij} e^{v_j^{\text{sc}}}, & \text{if } i \in J_{\varepsilon, \kappa}^{\mathbf{G}}, \end{cases} \quad (12)$$

and

$$\nu_j^{\text{sc}} = \begin{cases} e^{v_j^{\text{sc}}} \sum_{i=1}^n K_{ij} e^{u_i^{\text{sc}}}, & \text{if } j \in J_{\varepsilon, \kappa}, \\ \varepsilon \kappa \sum_{i=1}^n K_{ij} e^{u_i^{\text{sc}}}, & \text{if } j \in J_{\varepsilon, \kappa}^{\mathbf{G}}, \end{cases} = \begin{cases} \frac{\nu_j}{\kappa}, & \text{if } j \in J_{\varepsilon, \kappa}, \\ \varepsilon \kappa \sum_{i=1}^n K_{ij} e^{u_i^{\text{sc}}}, & \text{if } j \in J_{\varepsilon, \kappa}^{\mathbf{G}}. \end{cases} \quad (13)$$

By (12), we have

$$\begin{aligned} d_\rho(\mu, \mu^{\text{sc}}) &= \sum_{i=1}^n \mu_i^{\text{sc}} - \mu_i + \mu_i \log \left(\frac{\mu_i}{\mu_i^{\text{sc}}} \right) \\ &= \sum_{i \in I_{\varepsilon, \kappa}} (\kappa - 1) \mu_i - \mu_i \log(\kappa) + \sum_{i \in I_{\varepsilon, \kappa}^{\mathbf{G}}} \frac{\varepsilon}{\kappa} \sum_{j=1}^m K_{ij} e^{v_j^{\text{sc}}} - \mu_i + \mu_i \log \left(\frac{\mu_i}{\frac{\varepsilon}{\kappa} \sum_{j=1}^m K_{ij} e^{v_j^{\text{sc}}}} \right) \\ &= \sum_{i \in I_{\varepsilon, \kappa}} (\kappa - \log(\kappa) - 1) \mu_i + \sum_{i \in I_{\varepsilon, \kappa}^{\mathbf{G}}} \frac{\varepsilon}{\kappa} \sum_{j=1}^m K_{ij} e^{v_j^{\text{sc}}} - \mu_i + \mu_i \log \left(\frac{\mu_i}{\frac{\varepsilon}{\kappa} \sum_{j=1}^m K_{ij} e^{v_j^{\text{sc}}}} \right). \end{aligned}$$

Now by (8), we have in one hand

$$\begin{aligned} \sum_{i \in I_{\varepsilon, \kappa}^{\mathbf{G}}} \frac{\varepsilon}{\kappa} \sum_{j=1}^m K_{ij} e^{v_j^{\text{sc}}} &= \sum_{i \in I_{\varepsilon, \kappa}^{\mathbf{G}}} \frac{\varepsilon}{\kappa} \left(\sum_{j \in J_{\varepsilon, \kappa}} K_{ij} e^{v_j^{\text{sc}}} + \varepsilon \kappa \sum_{j \in J_{\varepsilon, \kappa}^{\mathbf{G}}} K_{ij} \right) \\ &\leq \sum_{i \in I_{\varepsilon, \kappa}^{\mathbf{G}}} \frac{\varepsilon}{\kappa} \left(m_b \max_{i,j} K_{ij} \frac{\max_{j \in J_{\varepsilon, \kappa}} \nu_j}{n \varepsilon K_{\min}} + (m - m_b) \varepsilon \kappa \max_{i,j} K_{ij} \right) \\ &\leq (n - n_b) \left(\frac{m_b \max_j \nu_j}{n \kappa K_{\min}} + (m - m_b) \varepsilon^2 \right). \end{aligned}$$

On the other hand, we get

$$\begin{aligned} \frac{\varepsilon}{\kappa} \sum_{j=1}^m K_{ij} e^{v_j^{\text{sc}}} &= \frac{\varepsilon}{\kappa} \left(\sum_{j \in J_{\varepsilon, \kappa}} K_{ij} e^{v_j^{\text{sc}}} + \varepsilon \kappa \sum_{j \in J_{\varepsilon, \kappa}^{\mathbf{G}}} K_{ij} \right) \\ &\geq m_b K_{\min} \frac{m \varepsilon^2 K_{\min} \min_{j \in J_{\varepsilon, \kappa}} \nu_j}{\kappa((n - n_b) m \varepsilon^2 K_{\min} + m \varepsilon^2 K_{\min} + n_b \kappa \max_{i \in I_{\varepsilon, \kappa}} \mu_i)} \\ &\quad + \varepsilon^2 (m - m_b) K_{\min} \\ &\geq \frac{m m_b \varepsilon^2 (K_{\min})^2 \min_{j \in J_{\varepsilon, \kappa}} \nu_j}{\kappa((n - n_b) m \varepsilon^2 K_{\min} + m \varepsilon^2 K_{\min} + n_b \kappa \max_{i \in I_{\varepsilon, \kappa}} \mu_i)} \\ &\quad + \varepsilon^2 (m - m_b) K_{\min} \\ &\geq \frac{m m_b \varepsilon^2 K_{\min}^2 \min_{j \in J_{\varepsilon, \kappa}} \nu_j}{\kappa((n - n_b) m \varepsilon^2 K_{\min} + m \varepsilon^2 K_{\min} + n_b \kappa \max_{i \in I_{\varepsilon, \kappa}} \mu_i)}. \end{aligned}$$

Then

$$\begin{aligned} \frac{1}{\frac{\varepsilon}{\kappa} \sum_{j=1}^m K_{ij} e^{v_j^{\text{sc}}}} &\leq \frac{\kappa((n - n_b) m \varepsilon^2 K_{\min} + m \varepsilon^2 K_{\min} + n_b \kappa \max_{i \in I_{\varepsilon, \kappa}} \mu_i)}{m m_b \varepsilon^2 K_{\min}^2 \min_{j \in J_{\varepsilon, \kappa}} \nu_j} \\ &\leq \frac{\kappa(n - n_b + 1)}{m_b K_{\min} \min_{j \in J_{\varepsilon, \kappa}} \nu_j} + \frac{n_b \kappa^2 \max_{i \in I_{\varepsilon, \kappa}} \mu_i}{m m_b \varepsilon^2 K_{\min}^2 \min_{j \in J_{\varepsilon, \kappa}} \nu_j}. \end{aligned}$$

It entails

$$\begin{aligned} \sum_{i \in I_{\varepsilon, \kappa}^{\mathbf{G}}} \frac{\varepsilon}{\kappa} \sum_{j=1}^m K_{ij} e^{v_j^{\text{sc}}} - \mu_i + \mu_i \log \left(\frac{\mu_i}{\frac{\varepsilon}{\kappa} \sum_{j=1}^m K_{ij} e^{v_j^{\text{sc}}}} \right) \\ \leq (n - n_b) \left(\frac{m_b}{n \kappa K_{\min}} + (m - m_b) \varepsilon^2 - \min_i \mu_i \right. \\ \left. + \max_i \mu_i \log \left(\frac{\kappa(n - n_b + 1) \max_i \mu_i}{m_b K_{\min} \min_{j \in J_{\varepsilon, \kappa}} \nu_j} + \frac{n_b \kappa^2 (\max_i \mu_i)^2}{m m_b \varepsilon^2 K_{\min}^2 \min_{j \in J_{\varepsilon, \kappa}} \nu_j} \right) \right). \end{aligned}$$

Therefore

$$d_\varrho(\mu, \mu^{\text{sc}}) \leq n_b c_\kappa \max_i \mu_i + (n - n_b) \left(\frac{m_b \max_j \nu_j}{n \kappa K_{\min}} + (m - m_b) \varepsilon^2 - \min_i \mu_i \right) \\ + \max_i \mu_i \log \left(\frac{\kappa(n - n_b + 1) \max_i \mu_i}{m_b K_{\min} \min_{j \in J_{\varepsilon, \kappa}} \nu_j} + \frac{n_b \kappa^2 (\max_i \mu_i)^2}{m m_b \varepsilon^2 K_{\min}^2 \min_{j \in J_{\varepsilon, \kappa}} \nu_j} \right).$$

Finally, by Lemma 2 we obtain

$$\|\mu - \mu^{\text{sc}}\|_1^2 \leq n_b c_\kappa \max_i \mu_i + 7(n - n_b) \left(\frac{m_b \max_j \nu_j}{n \kappa K_{\min}} + (m - m_b) \varepsilon^2 - \min_i \mu_i \right) \\ + \max_i \mu_i \log \left(\frac{\kappa(n - n_b + 1) \max_i \mu_i}{m_b K_{\min} \min_{j \in J_{\varepsilon, \kappa}} \nu_j} + \frac{n_b \kappa^2 (\max_i \mu_i)^2}{m m_b \varepsilon^2 K_{\min}^2 \min_{j \in J_{\varepsilon, \kappa}} \nu_j} \right).$$

Following the same lines as above, we also have

$$\|\nu - \nu^{\text{sc}}\|_1^2 \leq m_b c_{\frac{1}{\kappa}} \max_i \mu_i + 7(m - m_b) \left(\frac{n_b \kappa \max_i \mu_i}{m K_{\min}} + (n - n_b) \varepsilon^2 - \min_j \nu_j \right) \\ + \max_j \nu_j \log \left(\frac{(m - m_b + 1) \max_j \nu_j}{n_b \kappa K_{\min} \min_{i \in I_{\varepsilon, \kappa}} \mu_i} + \frac{m_b (\max_j \nu_j)^2}{n n_b \varepsilon^2 \kappa^2 K_{\min}^2 \min_{i \in I_{\varepsilon, \kappa}} \mu_i} \right).$$

To get the closed forms (9) and (10), we used the following facts:

Remark 1. We have $\log(1/K_{\min}^r) = r \|C\|_{\infty} / \eta$, for every $r \in \mathbb{N}$. Using (5), we further derive: $\varepsilon = \mathcal{O}((mnK_{\min}^2)^{-1/4})$, $\kappa = \mathcal{O}(\sqrt{m/(nc_{\mu\nu}K_{\min})})$, $\kappa^{-1} = \mathcal{O}(\sqrt{n/(mK_{\min}c_{\mu\nu})})$, $(\kappa/\varepsilon)^2 = \mathcal{O}(m^{3/2}/\sqrt{nK_{\min}}(c_{\mu\nu})^{3/2})$, and $(\varepsilon\kappa)^{-2} = \mathcal{O}(n^{3/2}/\sqrt{mK_{\min}}(c_{\mu\nu})^{3/2})$.

7.4 Proof of Proposition 3

We first define \tilde{K} a rearrangement of K with respect to the active sets $I_{\varepsilon, \kappa}$ and $J_{\varepsilon, \kappa}$ as follows:

$$\tilde{K} = \begin{bmatrix} K_{(I_{\varepsilon, \kappa}, J_{\varepsilon, \kappa})} & K_{(I_{\varepsilon, \kappa}, J_{\varepsilon, \kappa}^c)} \\ K_{(I_{\varepsilon, \kappa}^c, J_{\varepsilon, \kappa})} & K_{(I_{\varepsilon, \kappa}^c, J_{\varepsilon, \kappa}^c)} \end{bmatrix}.$$

Setting $\hat{\mu} = (\mu_{I_{\varepsilon, \kappa}}^\top, \mu_{I_{\varepsilon, \kappa}^c}^\top)^\top$, $\hat{\nu} = (\nu_{J_{\varepsilon, \kappa}}^\top, \nu_{J_{\varepsilon, \kappa}^c}^\top)^\top$ and for each vectors $u \in \mathbb{R}^n$ and $v \in \mathbb{R}^m$ we set $\hat{u} = (u_{I_{\varepsilon, \kappa}}^\top, u_{I_{\varepsilon, \kappa}^c}^\top)^\top$ and $\hat{v} = (v_{J_{\varepsilon, \kappa}}^\top, v_{J_{\varepsilon, \kappa}^c}^\top)^\top$. We then have

$$\Psi_{\varepsilon, \kappa}(u, v) = \mathbf{1}_n^\top \tilde{K}(\hat{u}, \hat{v}) \mathbf{1}_m - \kappa \hat{\mu}^\top \hat{u} - \kappa^{-1} \hat{\nu}^\top \hat{v},$$

and

$$\Psi(u, v) = \mathbf{1}_n^\top \tilde{K}(\hat{u}, \hat{v}) \mathbf{1}_m - \hat{\mu}^\top \hat{u} - \hat{\nu}^\top \hat{v},$$

where

$$\tilde{B}(\hat{u}, \hat{v}) = \Delta(e^{\hat{u}}) \tilde{K} \Delta(e^{\hat{v}}).$$

Let us consider the convex function

$$\langle \hat{u}, \hat{v} \rangle \mapsto \langle \mathbf{1}_n, \tilde{B}(\hat{u}, \hat{v}) \mathbf{1}_m \rangle - \langle \kappa \hat{u}, \tilde{B}(\hat{u}^{\text{sc}}, \hat{v}^{\text{sc}}) \mathbf{1}_m \rangle - \langle \kappa^{-1} \hat{v}, \tilde{B}(\hat{u}^{\text{sc}}, \hat{v}^{\text{sc}})^\top \mathbf{1}_n \rangle.$$

Gradient inequality of any convex function g at point x_o reads as $g(x_o) \geq g(x) + \langle \nabla g(x), x_o - x \rangle$, for all $x \in \text{dom}(g)$. Applying the latter fact to the above function at point (\hat{u}^*, \hat{v}^*) we obtain

$$\langle \mathbf{1}_n, \tilde{B}(\hat{u}^{\text{sc}}, \hat{v}^{\text{sc}}) \mathbf{1}_m \rangle - \langle \kappa \hat{u}^{\text{sc}}, \tilde{B}(\hat{u}^{\text{sc}}, \hat{v}^{\text{sc}}) \mathbf{1}_m \rangle - \langle \kappa^{-1} \hat{v}^{\text{sc}}, \tilde{B}(\hat{u}^{\text{sc}}, \hat{v}^{\text{sc}})^\top \mathbf{1}_n \rangle \\ - (\langle \mathbf{1}_n, \tilde{B}(\hat{u}^*, \hat{v}^*) \mathbf{1}_m \rangle - \langle \kappa \hat{u}^*, \tilde{B}(\hat{u}^{\text{sc}}, \hat{v}^{\text{sc}}) \mathbf{1}_m \rangle - \langle \kappa^{-1} \hat{v}^*, \tilde{B}(\hat{u}^{\text{sc}}, \hat{v}^{\text{sc}})^\top \mathbf{1}_n \rangle) \\ \leq \langle \hat{u}^{\text{sc}} - \hat{u}^*, (1 - \kappa) \tilde{B}(\hat{u}^{\text{sc}}, \hat{v}^{\text{sc}}) \mathbf{1}_m \rangle + \langle \hat{v}^{\text{sc}} - \hat{v}^*, (1 - \kappa^{-1}) \tilde{B}(\hat{u}^{\text{sc}}, \hat{v}^{\text{sc}})^\top \mathbf{1}_n \rangle.$$

Moreover,

$$\Psi_{\varepsilon, \kappa}(u^{\text{sc}}, v^{\text{sc}}) - \Psi(u^*, v^*) = \langle \mathbf{1}_n, \tilde{B}(\hat{u}^{\text{sc}}, \hat{v}^{\text{sc}}) \mathbf{1}_m \rangle - \langle \kappa \hat{u}^{\text{sc}}, \tilde{B}(\hat{u}^{\text{sc}}, \hat{v}^{\text{sc}}) \mathbf{1}_m \rangle - \langle \kappa^{-1} \hat{v}^{\text{sc}}, \tilde{B}(\hat{u}^{\text{sc}}, \hat{v}^{\text{sc}})^\top \mathbf{1}_n \rangle \\ - (\langle \mathbf{1}_n, \tilde{B}(\hat{u}^*, \hat{v}^*) \mathbf{1}_m \rangle - \langle \hat{u}^*, \tilde{B}(\hat{u}^{\text{sc}}, \hat{v}^{\text{sc}}) \mathbf{1}_m \rangle - \langle \hat{v}^*, \tilde{B}(\hat{u}^{\text{sc}}, \hat{v}^{\text{sc}})^\top \mathbf{1}_n \rangle) \\ + \langle \kappa \hat{u}^{\text{sc}} - \hat{u}^*, \tilde{B}(\hat{u}^{\text{sc}}, \hat{v}^{\text{sc}}) \mathbf{1}_m - \hat{\mu} \rangle + \langle \kappa^{-1} \hat{v}^{\text{sc}} - \hat{v}^*, \tilde{B}(\hat{u}^{\text{sc}}, \hat{v}^{\text{sc}})^\top \mathbf{1}_n - \hat{\nu} \rangle.$$

Hence,

$$\Psi_{\varepsilon, \kappa}(u^{\text{sc}}, v^{\text{sc}}) - \Psi(u^*, v^*) + (\langle \mathbf{1}_n, \tilde{B}(\hat{u}^*, \hat{v}^*) \mathbf{1}_m \rangle \\ - \langle \hat{u}^*, \tilde{B}(\hat{u}^{\text{sc}}, \hat{v}^{\text{sc}}) \mathbf{1}_m \rangle - \langle \hat{v}^*, \tilde{B}(\hat{u}^{\text{sc}}, \hat{v}^{\text{sc}})^\top \mathbf{1}_n \rangle) \\ - \langle \kappa \hat{u}^{\text{sc}} - \hat{u}^*, \tilde{B}(\hat{u}^{\text{sc}}, \hat{v}^{\text{sc}}) \mathbf{1}_m - \hat{\mu} \rangle - \langle \kappa^{-1} \hat{v}^{\text{sc}} - \hat{v}^*, \tilde{B}(\hat{u}^{\text{sc}}, \hat{v}^{\text{sc}})^\top \mathbf{1}_n - \hat{\nu} \rangle \\ \leq \langle \hat{u}^{\text{sc}} - \hat{u}^*, (1 - \kappa) \tilde{B}(\hat{u}^{\text{sc}}, \hat{v}^{\text{sc}}) \mathbf{1}_m \rangle + \langle \hat{v}^{\text{sc}} - \hat{v}^*, (1 - \kappa^{-1}) \tilde{B}(\hat{u}^{\text{sc}}, \hat{v}^{\text{sc}})^\top \mathbf{1}_n \rangle \\ + (\langle \mathbf{1}_n, \tilde{B}(\hat{u}^*, \hat{v}^*) \mathbf{1}_m \rangle - \langle \kappa \hat{u}^*, \tilde{B}(\hat{u}^{\text{sc}}, \hat{v}^{\text{sc}}) \mathbf{1}_m \rangle - \langle \kappa^{-1} \hat{v}^*, \tilde{B}(\hat{u}^{\text{sc}}, \hat{v}^{\text{sc}})^\top \mathbf{1}_n \rangle).$$

Then,

$$\begin{aligned}\Psi_{\varepsilon,\kappa}(u^{\text{sc}}, v^{\text{sc}}) - \Psi(u^*, v^*) &\leq \langle \dot{u}^{\text{sc}} - \dot{u}^*, (1 - \kappa)\tilde{B}(\dot{u}^{\text{sc}}, \dot{v}^{\text{sc}})\mathbf{1}_m \rangle + \langle \dot{v}^{\text{sc}} - \dot{v}^*, (1 - \kappa^{-1})\tilde{B}(\dot{u}^{\text{sc}}, \dot{v}^{\text{sc}})^\top \mathbf{1}_n \rangle \\ &\quad + (\langle \mathbf{1}_n, \tilde{B}(\dot{u}^*, \dot{v}^*)\mathbf{1}_m \rangle - \langle \kappa\dot{u}^*, \tilde{B}(\dot{u}^{\text{sc}}, \dot{v}^{\text{sc}})\mathbf{1}_m \rangle - \langle \kappa^{-1}\dot{v}^*, \tilde{B}(\dot{u}^{\text{sc}}, \dot{v}^{\text{sc}})^\top \mathbf{1}_n \rangle) \\ &\quad + \langle \kappa\dot{u}^{\text{sc}} - \dot{u}^*, \tilde{B}(\dot{u}^{\text{sc}}, \dot{v}^{\text{sc}})\mathbf{1}_m - \dot{\mu} \rangle + \langle \kappa^{-1}\dot{v}^{\text{sc}} - \dot{v}^*, \tilde{B}(\dot{u}^{\text{sc}}, \dot{v}^{\text{sc}})^\top \mathbf{1}_n - \dot{\nu} \rangle \\ &\quad - (\langle \mathbf{1}_n, \tilde{B}(\dot{u}^*, \dot{v}^*)\mathbf{1}_m \rangle - \langle \dot{u}^*, \tilde{B}(\dot{u}^{\text{sc}}, \dot{v}^{\text{sc}})\mathbf{1}_m \rangle - \langle \dot{v}^*, \tilde{B}(\dot{u}^{\text{sc}}, \dot{v}^{\text{sc}})^\top \mathbf{1}_n \rangle),\end{aligned}$$

which yields

$$\begin{aligned}\Psi_{\varepsilon,\kappa}(u^{\text{sc}}, v^{\text{sc}}) - \Psi(u^*, v^*) &\leq \langle \kappa\dot{u}^{\text{sc}} - \dot{u}^*, \tilde{B}(\dot{u}^{\text{sc}}, \dot{v}^{\text{sc}})\mathbf{1}_m - \dot{\mu} \rangle + \langle \kappa^{-1}\dot{v}^{\text{sc}} - \dot{v}^*, \tilde{B}(\dot{u}^{\text{sc}}, \dot{v}^{\text{sc}})^\top \mathbf{1}_n - \dot{\nu} \rangle \\ &\quad + (1 - \kappa)\langle \dot{u}^{\text{sc}}, \tilde{B}(\dot{u}^{\text{sc}}, \dot{v}^{\text{sc}})\mathbf{1}_m \rangle + (1 - \kappa^{-1})\langle \dot{v}^{\text{sc}}, \tilde{B}(\dot{u}^{\text{sc}}, \dot{v}^{\text{sc}})^\top \mathbf{1}_n \rangle.\end{aligned}$$

Applying Holder's inequality gives

$$\begin{aligned}\Psi_{\varepsilon,\kappa}(u^{\text{sc}}, v^{\text{sc}}) - \Psi(u^*, v^*) &\leq \|\kappa\dot{u}^{\text{sc}} - \dot{u}^*\|_\infty \|\tilde{B}(\dot{u}^{\text{sc}}, \dot{v}^{\text{sc}})\mathbf{1}_m - \dot{\mu}\|_1 + \|\kappa^{-1}\dot{v}^{\text{sc}} - \dot{v}^*\|_\infty \|\tilde{B}(\dot{u}^{\text{sc}}, \dot{v}^{\text{sc}})^\top \mathbf{1}_n - \dot{\nu}\|_1 \\ &\quad + (1 - \kappa)\langle \dot{u}^{\text{sc}}, \tilde{B}(\dot{u}^{\text{sc}}, \dot{v}^{\text{sc}})\mathbf{1}_m \rangle + (1 - \kappa^{-1})\langle \dot{v}^{\text{sc}}, \tilde{B}(\dot{u}^{\text{sc}}, \dot{v}^{\text{sc}})^\top \mathbf{1}_n \rangle \\ &\leq (\|\dot{u}^{\text{sc}} - \dot{u}^*\|_\infty + (1 - \kappa)\|\dot{u}^{\text{sc}}\|_\infty) \|\tilde{B}(\dot{u}^{\text{sc}}, \dot{v}^{\text{sc}})\mathbf{1}_m - \dot{\mu}\|_1 \\ &\quad + (\|\dot{v}^{\text{sc}} - \dot{v}^*\|_\infty + (\kappa^{-1} - 1)\|\dot{v}^{\text{sc}}\|_\infty) \|\tilde{B}(\dot{u}^{\text{sc}}, \dot{v}^{\text{sc}})^\top \mathbf{1}_n - \dot{\nu}\|_1 \\ &\quad + (1 - \kappa)\langle \dot{u}^{\text{sc}}, \tilde{B}(\dot{u}^{\text{sc}}, \dot{v}^{\text{sc}})\mathbf{1}_m \rangle + (\kappa^{-1} - 1)\langle \dot{v}^{\text{sc}}, \tilde{B}(\dot{u}^{\text{sc}}, \dot{v}^{\text{sc}})^\top \mathbf{1}_n \rangle\end{aligned}$$

where, in the last inequality, we use the facts that $\|\kappa\dot{u}^{\text{sc}} - \dot{u}^*\|_\infty \leq \|\dot{u}^{\text{sc}} - \dot{u}^*\|_\infty + (1 - \kappa)\|\dot{u}^{\text{sc}}\|_\infty$ and $\|\kappa^{-1}\dot{v}^{\text{sc}} - \dot{v}^*\|_\infty \leq \|\dot{v}^{\text{sc}} - \dot{v}^*\|_\infty + (\kappa^{-1} - 1)\|\dot{v}^{\text{sc}}\|_\infty$. Moreover, note that

$$\begin{cases} \|\dot{u}^{\text{sc}} - \dot{u}^*\|_\infty = \|u^{\text{sc}} - u^*\|_\infty, & \text{and } \begin{cases} \|\tilde{B}(\dot{u}^{\text{sc}}, \dot{v}^{\text{sc}})\mathbf{1}_m - \dot{\mu}\|_1 = \|B(u^{\text{sc}}, v^{\text{sc}})\mathbf{1}_m - \mu\|_1 = \|\mu^{\text{sc}} - \mu\|_1, \\ \|\tilde{B}(\dot{u}^{\text{sc}}, \dot{v}^{\text{sc}})^\top \mathbf{1}_n - \dot{\nu}\|_1 = \|B(u^{\text{sc}}, v^{\text{sc}})^\top \mathbf{1}_n - \nu\|_1 = \|\nu^{\text{sc}} - \nu\|_1. \end{cases} \\ \|\dot{v}^{\text{sc}} - \dot{v}^*\|_\infty = \|v^{\text{sc}} - v^*\|_\infty, \end{cases}$$

Then

$$\begin{aligned}\Psi_{\varepsilon,\kappa}(u^{\text{sc}}, v^{\text{sc}}) - \Psi(u^*, v^*) &\leq (\|u^{\text{sc}} - u^*\|_\infty + (1 - \kappa)\|u^{\text{sc}}\|_\infty) \|\mu^{\text{sc}} - \mu\|_1 \\ &\quad + (\|v^{\text{sc}} - v^*\|_\infty + (\kappa^{-1} - 1)\|v^{\text{sc}}\|_\infty) \|\nu^{\text{sc}} - \nu\|_1 \\ &\quad + (1 - \kappa)\langle u^{\text{sc}}, \mu^{\text{sc}} \rangle + (\kappa^{-1} - 1)\langle v^{\text{sc}}, \nu^{\text{sc}} \rangle \\ &\leq (\|u^{\text{sc}} - u^*\|_\infty + (1 - \kappa)\|u^{\text{sc}}\|_\infty) \|\mu^{\text{sc}} - \mu\|_1 \\ &\quad + (\|v^{\text{sc}} - v^*\|_\infty + (\kappa^{-1} - 1)\|v^{\text{sc}}\|_\infty) \|\nu^{\text{sc}} - \nu\|_1 \tag{14} \\ &\quad + (1 - \kappa)\|u^{\text{sc}}\|_\infty \|\mu^{\text{sc}}\|_1 + (1 - \kappa^{-1})\|v^{\text{sc}}\|_\infty \|\nu^{\text{sc}}\|_1.\end{aligned}$$

Next, we bound the two terms $\|u^{\text{sc}} - u^*\|_\infty$ and $\|v^{\text{sc}} - v^*\|_\infty$. If $r \in I_{\varepsilon,\kappa}^{\mathbb{C}}$, then we have

$$\begin{aligned}|(u^{\text{sc}})_r - u_r^*| &= \left| \log \left(\frac{\sum_{j=1}^m K_{rj} e^{v_j^*}}{\sum_{j=1}^m \frac{\kappa\mu_r}{m\varepsilon}} \right) \right| \\ &\stackrel{(*)}{\leq} \left| \log \left(\max_{1 \leq i \leq m} \frac{K_{rj} e^{v_j^*}}{\frac{\kappa\mu_r}{m\varepsilon}} \right) \right| \\ &\leq \left| \max_{1 \leq j \leq m} (v_j^* - \log(\frac{\kappa\mu_r}{m\varepsilon})) \right| \\ &\leq \|v^* - \log(\frac{\kappa\mu_r}{m\varepsilon})\|_\infty \\ &\leq \|v^* - v^{\text{sc}}\|_\infty + \log(\frac{m\varepsilon^2}{c_{\mu\nu}}).\end{aligned}$$

where the inequality $(*)$ comes from the fact that $\frac{\sum_{j=1}^n a_j}{\sum_{j=1}^n b_j} \leq \max_{1 \leq j \leq n} \frac{a_j}{b_j}$, $\forall a_j, b_j > 0$. Now, if $r \in I_{\varepsilon,\kappa}$, we get

$$|u_r^{\text{sc}} - u_r^*| = \left| \log \left(\frac{\kappa \sum_{j=1}^m K_{rj} e^{v_j^*}}{\sum_{j=1}^m K_{rj} e^{(v^{\text{sc}})_j}} \right) \right| \leq \left| \log \left(\frac{\sum_{j=1}^m K_{rj} e^{v_j^*}}{\sum_{j=1}^m K_{rj} e^{(v^{\text{sc}})_j}} \right) \right| \stackrel{(*)}{\leq} \|v^{\text{sc}} - v^*\|_\infty.$$

If $s \in J_{\varepsilon, \kappa}^{\mathbf{G}}$ then

$$\begin{aligned}
|v_s^{\text{sc}} - v_s^*| &= \left| \log(\varepsilon \kappa) - \log\left(\frac{\nu_s}{\sum_{i=1}^n K_{is} e^{u_i^*}}\right) \right| \\
&\leq \left| \log\left(\max_{1 \leq i \leq n} \frac{K_{is} e^{u_i^*}}{\frac{\nu_s}{n \kappa \varepsilon}}\right) \right| \\
&\stackrel{(*)}{\leq} \left| \max_{1 \leq i \leq n} (u_i^* - \log(\frac{\nu_s}{n \kappa \varepsilon})) \right| \\
&\leq \|u^* - \log(\frac{\nu_s}{n \kappa \varepsilon})\|_{\infty} \\
&\leq \|u^* - u^{\text{sc}}\|_{\infty} + \log\left(\frac{n \varepsilon^2}{c_{\mu\nu}}\right).
\end{aligned}$$

If $s \in J_{\varepsilon, \kappa}$ then

$$|v_s^{\text{sc}} - v_s^*| = \left| \log\left(\frac{\kappa \sum_{i=1}^m K_{ri} e^{u_i^*}}{\sum_{i=1}^m K_{ri} e^{(u^{\text{sc}})_i}}\right) \right| \leq \left| \log\left(\frac{\kappa \sum_{i=1}^m K_{ri} e^{v_j^*}}{\sum_{i=1}^m K_{ri} e^{(u^{\text{sc}})_i}}\right) \right| \stackrel{(*)}{\leq} \|u^{\text{sc}} - u^*\|_{\infty}.$$

Therefore, we obtain the following bound:

$$\begin{aligned}
\max\{\|u^* - u^{\text{sc}}\|_{\infty}, \|v^* - v^{\text{sc}}\|_{\infty}\} &\leq \max\left\{\|u^*\|_{\infty} + \|u^{\text{sc}}\|_{\infty} + \log\left(\frac{n \varepsilon^2}{c_{\mu\nu}}\right), \|v^*\|_{\infty} + \|v^{\text{sc}}\|_{\infty} + \log\left(\frac{m \varepsilon^2}{c_{\mu\nu}}\right)\right\} \\
&\leq 2\left(\|u^*\|_{\infty} + \|v^*\|_{\infty} + \|u^{\text{sc}}\|_{\infty} + \|v^{\text{sc}}\|_{\infty} + \log\left(\frac{(n \vee m) \varepsilon^2}{c_{\mu\nu}}\right)\right).
\end{aligned} \tag{15}$$

Now, Lemma 3.2 in [30] provides an upper bound for the ℓ_{∞} of the optimal solution pair (u^*, v^*) of problem (2) as follows: $\|u^*\|_{\infty} \leq A$ and $\|v^*\|_{\infty} \leq A$, where

$$A = \frac{\|C\|_{\infty}}{\eta} + \log\left(\frac{n \vee m}{c_{\mu\nu}^2}\right). \tag{16}$$

Plugging (15) and (16) in (14), we obtain

$$\begin{aligned}
\Psi_{\varepsilon, \kappa}(u^{\text{sc}}, v^{\text{sc}}) - \Psi(u^*, v^*) &\leq 2\left(A + \|u^{\text{sc}}\|_{\infty} + \|v^{\text{sc}}\|_{\infty} + \log\left(\frac{(n \vee m) \varepsilon^2}{c_{\mu\nu}}\right)\right) (\|\mu^{\text{sc}} - \mu\|_1 + \|\nu^{\text{sc}} - \nu\|_1) \\
&\quad + (1 - \kappa) (\|u^{\text{sc}}\|_{\infty} \|\mu^{\text{sc}}\|_1 + \|\mu^{\text{sc}} - \mu\|_1) \\
&\quad + (\kappa^{-1} - 1) (\|v^{\text{sc}}\|_{\infty} \|\nu^{\text{sc}}\|_1 + \|\nu^{\text{sc}} - \nu\|_1).
\end{aligned} \tag{17}$$

By Proposition 1, we have

$$\|u^{\text{sc}}\|_{\infty} \leq \log\left(\frac{\varepsilon}{\kappa} \vee \frac{1}{m \varepsilon K_{\min}}\right) \text{ and } \|v^{\text{sc}}\|_{\infty} \leq \log\left(\varepsilon \kappa \vee \frac{1}{n \varepsilon K_{\min}}\right)$$

and hence by Remark 1,

$$\|u^{\text{sc}}\|_{\infty} = \mathcal{O}\left(\log(n^{1/4}/(m K_{\min})^{3/4} c_{\mu\nu}^{1/4})\right) \text{ and } \|u^{\text{sc}}\|_{\infty} = \mathcal{O}\left(\log(m^{1/4}/(n K_{\min})^{3/4} c_{\mu\nu}^{1/4})\right).$$

Acknowledging that $\log(1/K_{\min}^2) = 2\|C\|_{\infty}/\eta$, we have

$$A + \|u^{\text{sc}}\|_{\infty} + \|v^{\text{sc}}\|_{\infty} + \log\left(\frac{(n \vee m) \varepsilon^2}{c_{\mu\nu}}\right) = \mathcal{O}\left(\frac{\|C\|_{\infty}}{\eta} + \log\left(\frac{(n \vee m)^2}{n m c_{\mu\nu}^{7/2}}\right)\right).$$

Letting $\Omega_{\kappa} := (1 - \kappa) (\|u^{\text{sc}}\|_{\infty} \|\mu^{\text{sc}}\|_1 + \|\mu^{\text{sc}} - \mu\|_1) + (\kappa^{-1} - 1) (\|v^{\text{sc}}\|_{\infty} \|\nu^{\text{sc}}\|_1 + \|\nu^{\text{sc}} - \nu\|_1)$. We have that

$$\begin{aligned}
\Omega_{\kappa} &= \mathcal{O}\left(\left(\frac{\|C\|_{\infty}}{\eta} + \log\left(\frac{1}{(nm)^{3/4} c_{\mu\nu}^{1/2}}\right)\right) \left((1 - \kappa) (\|\mu^{\text{sc}}\|_1 + \|\mu^{\text{sc}} - \mu\|_1) + (\kappa^{-1} - 1) (\|\nu^{\text{sc}}\|_1 + \|\nu^{\text{sc}} - \nu\|_1)\right)\right) \\
&= \mathcal{O}\left(\left(\frac{\|C\|_{\infty}}{\eta} + \log\left(\frac{(n \vee m)^2}{n m c_{\mu\nu}^{7/2}}\right)\right) \left((1 - \kappa) \|\mu^{\text{sc}}\|_1 + (\kappa^{-1} - 1) \|\nu^{\text{sc}}\|_1 + \kappa^{-1} - \kappa\right)\right).
\end{aligned}$$

Hence, we arrive at

$$\Psi_{\varepsilon, \kappa}(u^{\text{sc}}, v^{\text{sc}}) - \Psi(u^*, v^*) = \mathcal{O}(R(\|\mu - \mu^{\text{sc}}\|_1 + \|\nu - \nu^{\text{sc}}\|_1 + \omega_{\kappa})).$$

□

Note that ω_{κ} tends to zero as (n_b, m_b) tends to (n, m) (i.e., $\kappa \rightarrow 1$). To more characterize ω_{κ} , the following lemma expresses an upper bound with respect to ℓ_1 -norm of μ^{sc} and ν^{sc} .

Lemma 3. Let (u^{sc}, v^{sc}) be an optimal solution of problem (6). Then one has

$$\|\mu^{sc}\|_1 = \mathcal{O}\left(\frac{n_b\sqrt{m}}{\sqrt{n}K_{\min}c_{\mu\nu}} + (n - n_b)\left(\frac{m_b}{\sqrt{nm}c_{\mu\nu}K_{\min}^{3/2}} + \frac{m - m_b}{\sqrt{nm}K_{\min}}\right)\right), \quad (18)$$

and

$$\|\nu^{sc}\|_1 = \mathcal{O}\left(\frac{m_b\sqrt{n}}{\sqrt{m}K_{\min}c_{\mu\nu}} + (m - m_b)\left(\frac{n_b}{\sqrt{nm}c_{\mu\nu}K_{\min}^{3/2}} + \frac{n - n_b}{\sqrt{nm}K_{\min}}\right)\right). \quad (19)$$

Proof. Using inequality (8), we obtain

$$\begin{aligned} \|\mu^{sc}\|_1 &= \sum_{i \in I_{\varepsilon, \kappa}} \mu_i^{sc} + \sum_{i \in I_{\varepsilon, \kappa}^{\mathfrak{G}}} \mu_i^{sc} \\ &\stackrel{(12)}{=} \kappa \|\mu_{I_{\varepsilon, \kappa}}^{sc}\|_1 + \frac{\varepsilon}{\kappa} \sum_{i \in I^{\mathfrak{G}}} \left(\sum_{j \in J_{\varepsilon, \kappa}} K_{ij} e^{v_j^{sc}} + \varepsilon \kappa \sum_{j \in J_{\varepsilon, \kappa}^{\mathfrak{G}}} K_{ij} \right) \\ &\stackrel{(8)}{\leq} \kappa \|\mu_{I_{\varepsilon, \kappa}}^{sc}\|_1 + (n - n_b) \left(\frac{m_b \max_{j \in J_{\varepsilon, \kappa}} \nu_j}{n \kappa K_{\min}} + (m - m_b) \varepsilon^2 \right). \end{aligned}$$

Using Remark 1, we get the desired closed form in (18). Similarly, we can prove the same statement for $\|\nu^{sc}\|_1$. \square

7.5 Additional experimental results

Experimental setup. All computations have been run on each single core of an Intel Xeon E5-2630 processor clocked at 2.4 GHz in a Linux machine with 144 Gb of memory.

On the use of a constrained L-BFGS-B solver. It is worth to note that standard Sinkhorn's alternating minimization cannot be applied for the constrained screened dual problem (6). This appears more clearly while writing its optimality conditions (see Equations (12) and (13)). We resort to a L-BFGS-B algorithm to solve the constrained convex optimization problem on the screened variables (6), but any other efficient solver (e.g., proximal based method or Newton method) could be used. The choice of the starting point for the L-BFGS-B algorithm is given by the solution of the RESTRICTED SINKHORN method (see Algorithm 2), which is a Sinkhorn-like algorithm applied to the active dual variables. While simple and efficient the solution of this RESTRICTED SINKHORN algorithm does not satisfy the lower bound constraints of Problem (6). We further note that, as for the SINKHORN algorithm, our SCREENKHORN algorithm can be accelerated using a GPU implementation² of the L-BFGS-B algorithm [15].

Algorithm 2: RESTRICTED SINKHORN

1. **set:** $\bar{f}_u = \varepsilon \kappa c(K_{I_{\varepsilon, \kappa}, J_{\varepsilon, \kappa}^{\mathfrak{G}}}), \bar{f}_v = \varepsilon \kappa^{-1} r(K_{I_{\varepsilon, \kappa}^{\mathfrak{G}}, J_{\varepsilon, \kappa}})$;
 2. **for** $t = 1, 2, 3$ **do**

$$\left[\begin{array}{l} f_v^{(t)} \leftarrow K_{I_{\varepsilon, \kappa}, J_{\varepsilon, \kappa}}^{\top} u + \bar{f}_v; \\ v^{(t)} \leftarrow \frac{\nu_{J_{\varepsilon, \kappa}}}{\kappa f_v^{(t)}}; \\ f_u^{(t)} \leftarrow K_{I_{\varepsilon, \kappa}, J_{\varepsilon, \kappa}} v + \bar{f}_u; \\ u^{(t)} \leftarrow \frac{\kappa \mu_{I_{\varepsilon, \kappa}}}{f_u^{(t)}}; \\ u \leftarrow u^{(t)}, v \leftarrow v^{(t)}; \end{array} \right.$$
 3. **return** $(u^{(t)}, v^{(t)})$
-

Comparison with other solvers. We have considered experiments with GREENKHORN algorithm [3] but the implementation in POT library and our Python version of Matlab Altschuler's Greenkhorn code³ were not competitive with SINKHORN. Hence, for both versions, SCREENKHORN is more competitive than GREENKHORN. The computation time gain reaches an order of 30 when comparing our method with GREENKHORN while SCREENKHORN is almost 2 times faster than SINKHORN.

²<https://github.com/nepluno/lbfgsb-gpu>

³<https://github.com/JasonAltschuler/OptimalTransportNIPS17>

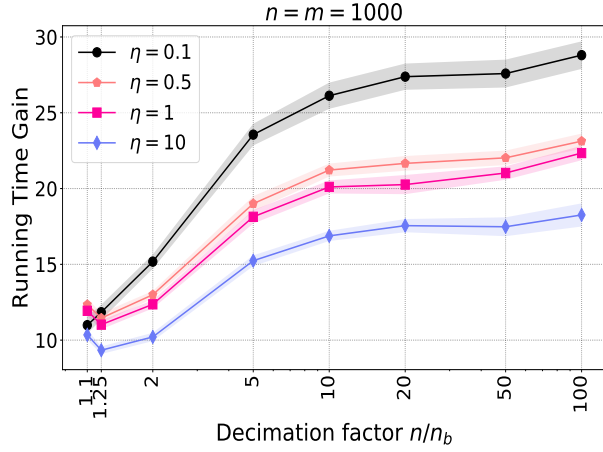


Figure 6: $\frac{T_{\text{GREENKHORN}}}{T_{\text{SCREENKHORN}}}$: Running time gain for the toy problem (see Section 5.2) as a function of the data decimation factor in SCREENKHORN, for different settings of the regularization parameter η .

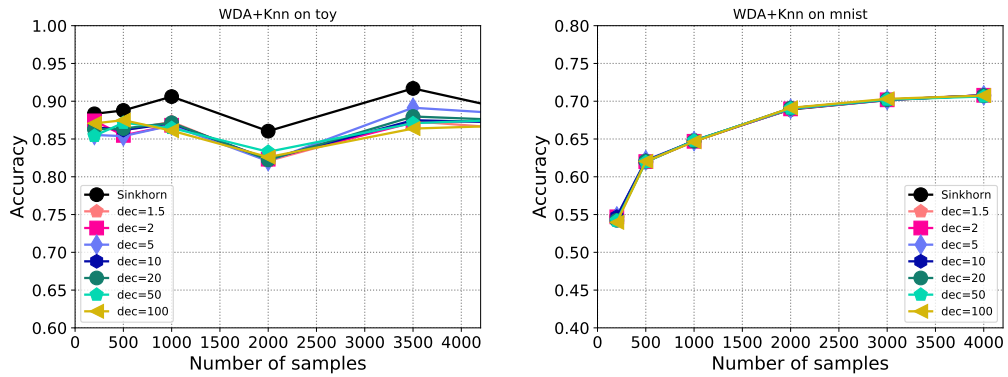


Figure 7: Accuracy of a 1-nearest-neighbour after WDA for the (left) toy problem and, (right) MNIST). We note a slight loss of performance for the toy problem, whereas for MNIST, all approaches yield the same performance.

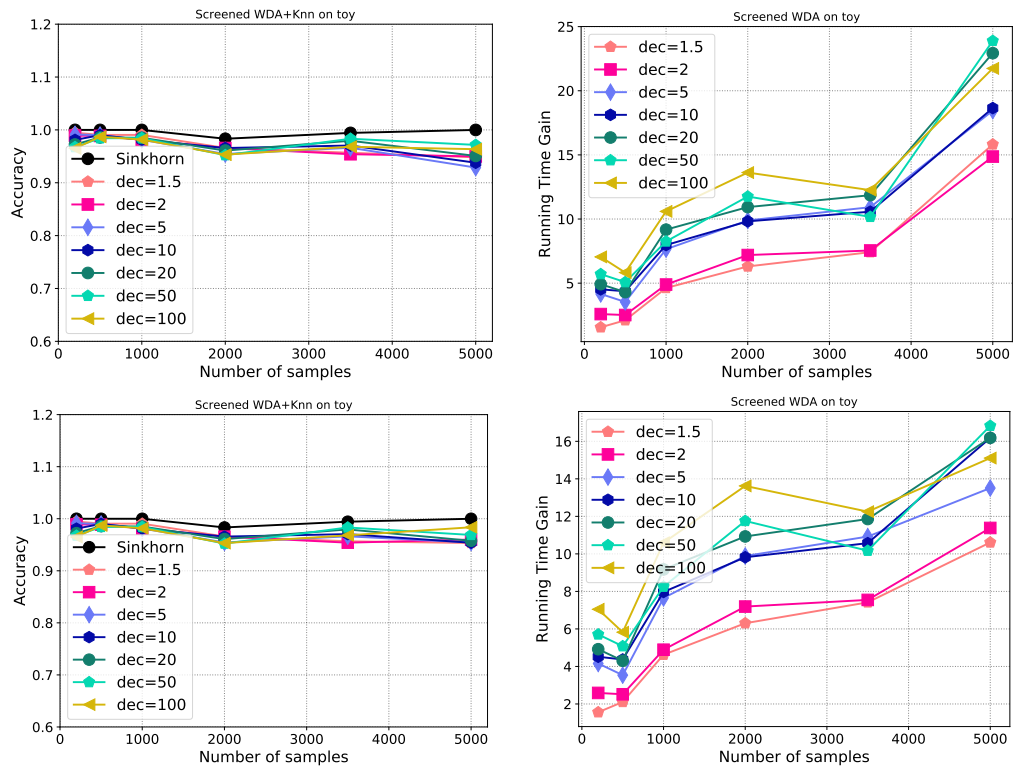


Figure 8: (top-left) Accuracy and (bottom-right) computational time gain on the toy dataset for $\eta = 0.1$ and 1-nearest-neighbour. (bottom) accuracy and gain but for a 5-nearest-neighbour. We can note that a slight loss of performances occur for larger training set sizes especially for 1-nearest-neighbour. Computational gains increase with the dataset size and are on average of the order of magnitude.

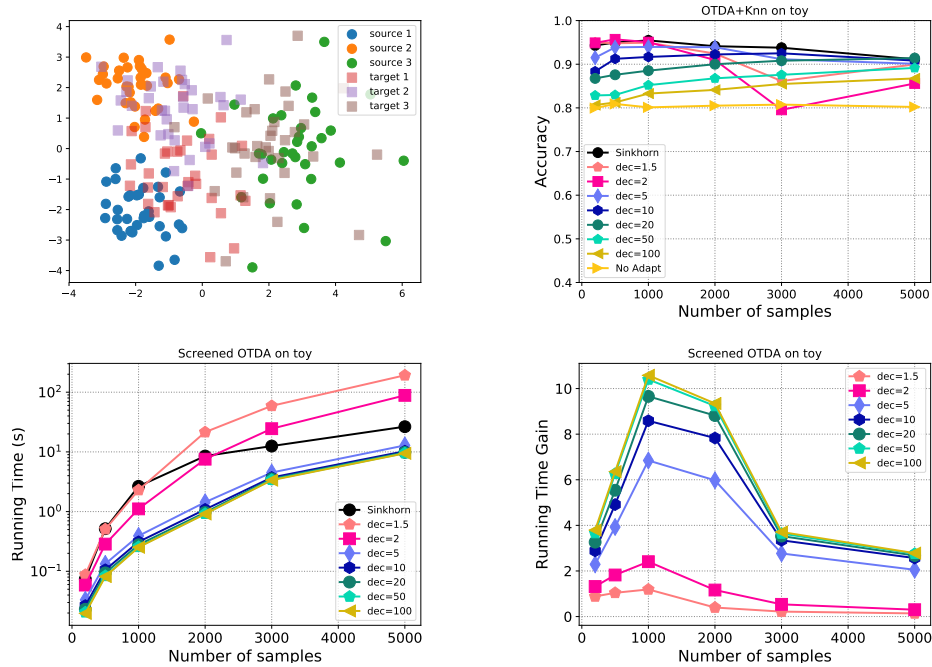


Figure 9: OT Domain Adaptation on a 3-class Gaussian toy problem. (top-left) Examples of source and target samples. (top-right) Evolution of the accuracy of a 1-nearest-neighbour classifier with respect to the number of samples. (bottom-left) Running time of the SINKHORN and SCREENKHORN for different decimation factors. (bottom-right). Gain in computation time. This toy problem is a problem in which classes are overlapping and distance between samples are rather limited. According to our analysis, this may be a situation in which SCREENKHORN may result in smaller computational gain. We can remark that with respect to the accuracy SCREENKHORN with decimation factors up to 10 are competitive with SINKHORN, although a slight loss of performance. Regarding computational time, for this example, small decimation factors does not result in gain. However for above 5-factor decimation, the gain goes from 2 to 10 depending on the number of samples.

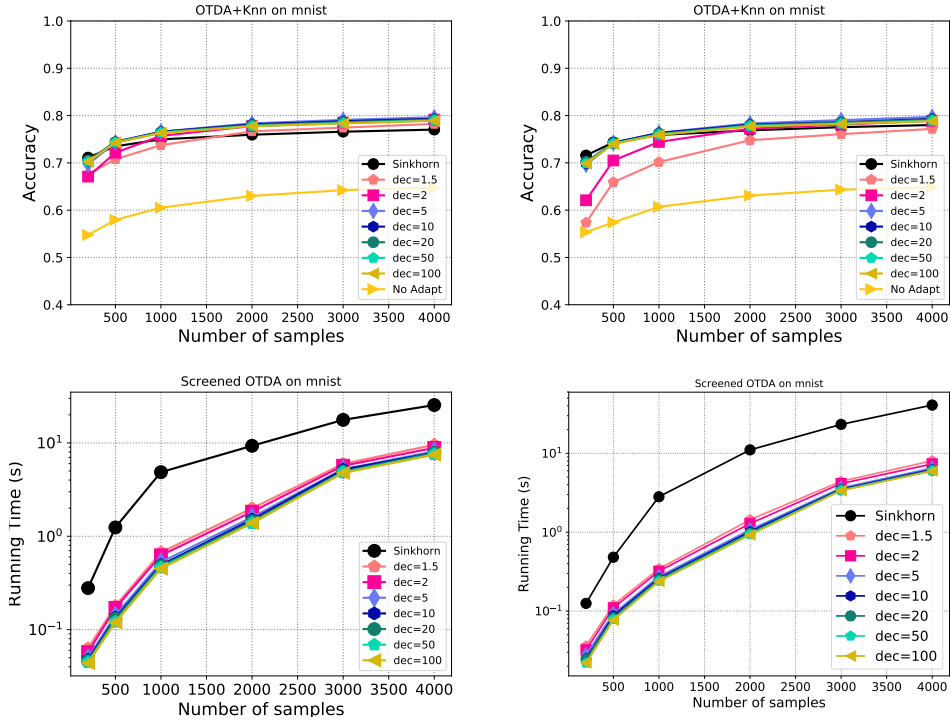


Figure 10: OT Domain adaptation MNIST to USPS : (top) Accuracy and (bottom) running time of SINKHORN and SCREENKHORN for hyperparameter of the $\ell_{p,1}$ regularizer (left) $\lambda = 1$ and (right) $\lambda = 10$. Note that this value impacts the ground cost of each Sinkhorn problem involved in the iterative algorithm. The accuracy panels also report the performance of a 1-NN when no-adaptation is performed. We remark that the strenght of the class-based regularization has influence on the performance of SCREENKHORN given a decimation factor. For small value on the left, SCREENKHORN slightly performs better than SINKHORN, while for large value, some decimation factors leads to loss of performances. Regarding, running time, we can note that SINKHORN is far less efficient than SCREENKHORN with an order of magnitude for intermediate number of samples.

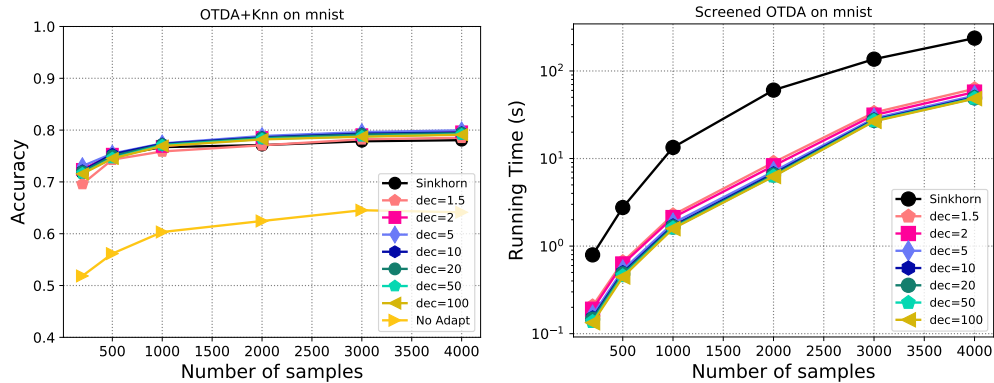


Figure 11: OT Domain adaptation MNIST to USPS : (left) Accuracy and (right) running time of SINKHORN and SCREENKHORN for the best performing (on average of 10 trials) hyperparameter $\ell_{p,1}$ chosen among the set $\{0.1, 1, 5, 10\}$. We can note that in this situation, there is not loss of accuracy while our SCREENKHORN is still about an order of magnitude more efficient than Sinkhorn.